Title

Short-term variability in euphotic zone biogeochemistry and primary productivity at Station ALOHA: A case study of summer 2012

Journal

Global Biogeochemical Cycles, 29(8)

ISSN

0886-6236

Authors

Wilson, Samuel T
Barone, Benedetto
Ascani, Francois
et al.

Publication Date

2015-08-01

DOI

10.1002/2015gb005141

Peer reviewed

Short-term variability in euphotic zone biogeochemistry and primary productivity at Station ALOHA: A case study of summer 2012

Samuel T. Wilson*[1,2], Benedetto Barone[1,2], Francois Ascani[1,3], Robert R. Bidigare[1,4], Matthew J. Church[1,2], Daniela A. del Valle[1,2], Sonya T. Dyhrman[1,5], Sara Ferrón[1,2], Jessica N. Fitzsimmons[1,6], Laurie W. Juranek[7], Zbigniew S. Kolber[1,8], Ricardo M. Letelier[1,7], Sandra Martínez-Garcia[1,2], David P. Nicholson[1,9], Kelvin J. Richards[1], Yoshimi M. Rii[1,2], Mónica Rouco[1,5], Donn A. Viviani[1,2], Angelicque E. White[1,7], Jonathan P. Zehr[1,8] and David M. Karl[1,2]

[1]Daniel K. Inouye Center for Microbial Oceanography: Research and Education (C-MORE), University of Hawai‘i at Manoa, Honolulu, Hawai‘i, USA.

[2] Department of Oceanography, University of Hawai‘i at Manoa, Honolulu, Hawai‘i, USA.

[3]current address: Marine Science Department, University of Hawaii at Hilo, Hilo, USA.

[4]Hawaii Institute of Marine Biology, University of Hawai‘i, Kaneohe, Hawai‘i, USA.

[5]Department of Earth and Environmental Sciences and the Lamont-Doherty Earth Observatory, Columbia University, Palisades, New York, USA

[6]current address: Institute of Marine and Coastal Sciences, Rutgers University, New Brunswick, New Jersey, USA

[7]College of Earth, Ocean, and Atmospheric Sciences, Oregon State University, Corvallis, Oregon, USA

[8]Department of Ocean Sciences, University of California, Santa Cruz, California, USA

[9]Marine Chemistry and Geochemistry Department, Woods Hole Oceanographic Institution, Woods Hole, Massachusetts, USA

*corresponding author. Email: stwilson@hawaii.edu Tel: 808-956-0573.

KEY POINTS

Biogeochemistry of oligotrophic gyres can vary on time-scales from days to weeks

A period of sustained net heterotrophy was observed during August 2012

A low surface salinity feature propagated through the field site

ABSTRACT

Time-series observations are critical to understanding the structure, function, and dynamics of marine ecosystems. The Hawaii Ocean Time-series (HOT) program has maintained near-monthly sampling at Station ALOHA (22° 45′N, 158° 00′W) in the oligotrophic North Pacific Subtropical Gyre (NPSG) since 1988 and identified ecosystem variability over seasonal to interannual time-scales. To further extend the temporal resolution of these near-monthly time-series observations, an extensive field campaign was conducted during July-September 2012 at Station ALOHA with near-daily sampling of upper water-column biogeochemistry, phytoplankton abundance, and activity. The resulting dataset provides biogeochemical measurements at high temporal resolution and documented two important events at Station ALOHA: (1) a prolonged period of low productivity when net community production in the mixed layer shifted to a net heterotrophic state and (2) detection of a distinct sea-surface salinity minimum feature which was prominent in the upper water-column (0–50 m) for a period of approximately 30 days. The shipboard observations during July-September 2012 were supplemented with *in situ* measurements provided by Seagliders, profiling floats, and remote satellite observations that together revealed the extent of the low productivity and the sea-surface salinity minimum feature in the NPSG.

1. Introduction

Understanding ocean ecosystems requires the collection of long-term, ecological time-series data at multiple locations in the world's oceans. The Hawaii Ocean Time-series (HOT) program [*Karl and Lukas*, 1996] has been sampling Station (Stn) ALOHA, situated in the North Pacific Subtropical Gyre (NPSG) at 22° 45′N, 158° 00′W, since October 1988, maintaining the original research objectives to observe and interpret physical and biogeochemical variability in the NPSG ecosystem [*Church et al*., 2013]. The scientific rationale and foresight to situate an oceanographic time-series program in the relatively stable oligotrophic gyre ecosystem to observe changes over seasonal and decadal timescales has proven to be valuable [*Venrick*, 1995]. Near-monthly hydrographic and biogeochemical observations have documented ecosystem variability over timescales ranging from interannual *e.g*. increasing oceanic CO_2 inventories [*Keeling et al*., 2004; *Dore et al*., 2009], climate-related biological changes [*Corno et al*., 2007; *Bidigare et al*., 2009] to seasonal cycles of phytoplankton productivity [*Letelier et al*., 1996; *Quay et al*., 2010], nitrogen fixation [*Church et al*., 2009], and the downward flux of particulate organic matter [*Karl et al*., 2012].

Augmentation of shipboard time-series observations with higher resolution *in situ* observations and experimentation has provided new insight into spatiotemporal variability in the open ocean. Recent oceanographic fieldwork in the oligotrophic NPSG has identified pelagic ecosystem variability not captured by the monthly sampling maintained by the HOT program. Recent examples of such field-based research include characterization of phytoplankton blooms [*Fong et al*., 2008; *Villareal et al*., 2012], eddy-driven export of plankton biomass [*Guidi et al*., 2012], and the vertical entrainment of nutrients into the lower regions of euphotic zone [*Johnson et al*., 2010; *Ascani et al*., 2013]. However these oceanographic measurements differ from the

Eulerian sampling strategy of the upper water-column maintained by the HOT program and until now high-resolution fixed-point observations of hydrographic and biogeochemical parameters during an entire season has not been achieved. Accomplishing this goal would help resolve the connections between biological and physical variability and identify the propagation of individual features and their associated biogeochemical properties through the study site which may otherwise be misinterpreted as temporal variability [*McGillicuddy*, 2001; *Karl, et al*., 2002; *Martin*, 2003].

In summer 2012, an extensive field campaign designed to improve the temporal resolution of upper water-column hydrographic and biogeochemical measurements in the NPSG was conducted by the Center for Microbial Oceanography: Research and Education (C-MORE). The upper ocean during the summer months, which vary in definition but broadly extend from June to September, is characterized by relatively shallow mixed layers, elevated daily light flux, low nutrient inventories, and episodic phytoplankton blooms that include diatoms in conjunction with nitrogen (N_2)-fixing cyanobacteria or solely N_2-fixing microorganisms (*e.g. Trichodesmium* spp.) [*Dore et al*., 2008; *Church et al*., 2009; *Wilson et al*., 2013]. It is during the summer period that an export pulse of sinking particulate material from the euphotic zone usually occurs [*Karl et al*., 2012] indicating a transient disconnect between production and consumption mechanisms. In the oligotrophic gyres, photosynthesis and respiration are generally tightly coupled with a resulting net metabolic balance slightly in favor of autotrophic [*Williams et al*., 2013] although net heterotrophic conditions have also been inferred [*Duarte et al*., 2013]. The metabolic balance, in terms of oxygen (O_2) and carbon (C), is represented by the residual between gross primary production (GPP) and community respiration (CR), referred to as net community

production (NCP). NCP is a small, yet critical term in the global carbon cycle as it represents the biologically produced carbon available for export from the upper ocean [*Emerson*, 2014].

This paper reports the hydrographic and biogeochemical conditions of the upper water-column at Stn ALOHA between July-September 2012. A striking observation during this period was the absence of any prolonged increase in phytoplankton biomass or bloom activity that is often observed during the summer time in the NPSG. Instead, anomalously low values of phytoplankton abundance and a period of net heterotrophy were recorded. In the absence of local or regional physical forcing mechanisms, we have identified several indicators of ecosystem-scale forcing which potentially contributed to this period of net heterotrophy. A separate hydrographic phenomenon, described as a 'sea-surface salinity minimum' was also observed and characterized. The low salinity water was associated with anomalously low concentrations of particulate material and phytoplankton. The daily measurements collected in this study are placed within the context of the 1988–2011 time-series climatology provided by the HOT program's measurements at Stn ALOHA. Ultimately the high-resolution Eulerian observations revealed the day-to-day biogeochemical variability of the upper water-column and identified hydrographic features that impact this open ocean oligotrophic habitat.

2. Materials and methods

2.1 Field operations and sampling

During 2012, a series of C-MORE-sponsored oceanographic expeditions collectively known as Hawaii Ocean Experiment: DYnamics of Light And Nutrients (HOE DYLAN) conducted operations at Stn ALOHA onboard the R/V *Kilo Moana* (Table 1). Three major expeditions covered a period from 8–28 July (KM1215), 5–14 August (KM1217), and 22 August to 11

September 2012 (KM1219). These C-MORE cruises were interspersed with monthly HOT program cruises (Table 1).

To characterize the upper water-column, vertical profiles of hydrographic parameters were conducted every 4 h during the three major cruises, typically to a depth of 400 m with a deeper cast extending to 1000 m conducted at 0800 hrs daily. The conductivity-temperature-depth (CTD) package (SBE 911Plus, SeaBird) was attached to a 24 x 12 L Niskin bottle rosette that also incorporated fluorescence, oxygen (O_2), and *in situ* ultraviolet spectrophotometer (ISUS, version 3, Satlantic) sensors. The conductivity, fluorescence, and O_2 sensors were calibrated using discrete measurements of salinity [*Bingham and Lukas,* 1996], fluorometric analysis of chlorophyll *a* and phaeopigments [*Strickland and Parsons,* 1972], and dissolved O_2 [*Carritt and Carpenter,* 1966], respectively. The mixed layer depth (MLD) was calculated based on a seawater density anomaly of 0.125 kg m^{-3} from the sea-surface.

During May through October 2012, a continuous traverse of a 50 km by 50 km 'bowtie'-shaped formation which extended from Stn ALOHA to the northeast was maintained by Seaglider operations. Each Seaglider cycle reached a maximum depth of 800 m, lasted approximately 6 h, and extended a horizontal distance of 3–5 km between surfacing. The bowtie formation was completed approximately every 2 weeks, allowing for calibration with shipboard measurements when the Seaglider traversed through Stn ALOHA. The Seaglider was equipped with a CTD package (Seabird) and sensors for O_2 (Seabird SBE-43 and Aanderaa Optode 3830), fluorescence, and optical backscatter (WET Labs) [*Eriksen et al*., 2001].

2.2 Biogeochemical analyses

141 The CTD casts conducted every 4 h were sampled systematically to determine the
142 hydrographic and biogeochemical properties of the water-column. The biogeochemical
143 properties of the water-column (nutrients, particulates, pigments) were sampled by conducting
144 vertical profiles at least every 3 days from discrete depths of 5, 25, 45, 75, 100, 125, 150 and
145 175 m. The vertical profiles were supplemented by higher temporal resolution sampling at
146 targeted depth horizons, e.g. at 25 m within the mixed layer. To ensure consistency of
147 measurements at Stn ALOHA, the majority of sampling and analytical protocols were identical
148 to those employed by the HOT program (http://hahana.soest.hawaii.edu/index.html). In brief,
149 nutrient analysis which included nitrite (NO_2^-) plus nitrate (NO_3^-) and phosphate was performed
150 on land using a Bran+Luebbe Autoanalyzer III. $NO_2^- + NO_3^-$ was also determined using the
151 chemiluminescence method for samples collected from 0–175 m as this method has an improved
152 detection limit of 1 nmol L^{-1} [*Dore and Karl,* 1996]. Seawater samples for particulate carbon
153 (PC) and particulate nitrogen (PN) were collected onto combusted 25 mm diameter Whatman
154 glass fiber filters (GF/F). The filters were stored frozen until analyzed using an Exeter CE-440
155 CHN elemental analyzer (Exeter Analytical, UK).
156 Phytoplankton pigments were analyzed using high performance liquid chromatography
157 (HPLC) as described by *Bidigare et al*., [2005]. Six diagnostic biomarker pigments
158 representative of the major phytoplankton taxa are reported which include fucoxanthin, 19′-
159 hexanoyloxyfucoxanthin, 19′-butanoyloxyfucoxanthin, zeaxanthin, divinylchlorophyll *a*, and
160 monovinylchlorophyll *a*. Sample volumes consisted of 2–4 L captured onto Whatman GF/F
161 filters, wrapped in foil, flash frozen and stored at -80°C. Pigments were extracted in 3 ml of
162 100% acetone in the dark at 4°C for 12 h followed by vortexing, centrifugation, and subsequent
163 analysis using a Varian 9012 HPLC system.

To characterize the N_2-fixing microorganisms, the *nifH* gene which encodes a subunit of the nitrogenase enzyme was quantified using quantitative PCR (qPCR). The groups of diazotrophs targeted included UCYN-A, *Crocosphaera* spp., *Trichodesmium* spp., and two types of heterocystous cyanobacteria that form symbioses with diatoms. Discrete seawater samples (2–4 L) were collected using the CTD-rosette, filtered using a peristaltic pump onto 10 µm polyester (GE Osmotics, Minnetonka, MN) and 0.2 µm Supor (Cole Parmer, Vernon Hills, IL) filters in series, frozen in liquid nitrogen, and stored at -80°C until processed. The DNA extraction was conducted using published protocols [*Moisander et al*., 2008] and the qPCR analyses conducted as previously described [*Goebel et al*., 2010].

Four independent shipboard measurements of productivity were conducted during July-September, although not all measurements extended for the entire period. Productivity measurements included the assimilation of ^{14}C-labeled bicarbonate ($NaH^{14}CO_3$) into particulate matter [*Letelier et al*., 1996], active fluorescence using fast repetition rate fluorometry (FRRF) [*Kolber and Falkowski*, 1993], and two dissolved gas measurements: triple O_2 isotope ($^{17}\Delta$) abundance to derive gross primary production [*Luz and Barkan*, 2000] and ratios of O_2/Ar to derive Net Community Production (NCP) [*Kaiser et al*., 2005]. Seawater samples for ^{14}C assimilation were collected pre-dawn at 0400 hrs, dissolved O_2/Argon (O_2/Ar) and triple O_2 isotope ($^{17}\Delta$) were collected at 0800 hrs, and FRRF was collected at 1600 hrs. Due to the diel variability in O_2 concentrations resulting from biological activity [*Hamme et al*., 2012; *Tortell et al*., 2014], calculation of NCP from instantaneous measurements of O_2/Ar in the early morning may result in an underestimation of NCP at Stn ALOHA by up to 20% compared to the daily mean rate [Ferrón *et al.*, 2015.]. Since our samples for O_2/Ar analysis were collected at 0800 hrs when rates of NCP are at their lowest, our measurements represent a lower estimate of NCP.

187 For the measurements of ^{14}C incorporation, seawater was collected at 0400 hrs from a depth
188 of 25 m into 500 ml acid-washed polycarbonate bottles in triplicate, spiked with $NaH^{14}CO_3$, and
189 incubated on-deck over the full daylight period [*Letelier et al*., 1996]. The on-deck incubators
190 were screened to the light levels equivalent to a depth of 25 m in the water-column using blue
191 acrylic shielding and flow-through surface seawater to maintain temperature. Sampling
192 protocols for ^{14}C assimilation measurements were identical for HOT and C-MORE cruises,
193 except the sample incubations were conducted *in situ* during the HOT expeditions rather than on-
194 deck incubators. To quantify ^{14}C assimilation, seawater was filtered onto 25 mm diameter
195 Whatman GF/F filters and placed into scintillation vials. After acidifying with 1 mL of 2 M HCl
196 and venting for 24 h to remove inorganic ^{14}C, 10 mL of scintillation cocktail (UltimaGold LLT,
197 PerkinElmer) was added to each vial and the radioactivity counted on a Packard liquid
198 scintillation counter (TriCarb2770TR/LT) and quench corrected using internal protocols. Rates
199 of ^{14}C incorporation (^{14}C-PP) are reported per day and represent the net incorporation of carbon
200 into particulate matter during the daylight period.
201 FRRF measurements were conducted on the ship's underway seawater system and from
202 vertical CTD-hydrocasts conducted daily at noon. The FRRF instrument was operated with a
203 broad-band excitation source in the 430–545 nm range. The FRRF-based estimates of primary
204 production (FRRF-PP) rates were calculated at time intervals of 15 min using the deckboard
205 PAR data, with the light propagation along the water-column based on light attenuation
206 coefficient provided by daily measurements of a hyperspectral radiometer (Satlantic). These
207 rates were integrated over a 24 h period using first-order interpolation to provide daily rates of
208 FRRF-PP. The rates of FRRF-PP were calculated according to *Suggett et al*. [2003] assuming 8

209 moles of quanta/mol O_2, and an average size of the photosynthetic unit of 500
210 (chlorophyll:reaction center).

211 The O_2/Ar measurements were conducted by filling 12 mL vials (Exetainer, Labco Ltd),
212 preserving with mercuric chloride ($HgCl_2$), and analyzing the O_2/Ar ratios using a membrane
213 inlet mass spectrometer (MIMS) [*Kana et al*., 1994]. Reference measurements consisted of
214 filtered (0.2 µm) surface seawater and the analytical temperature for reference seawater and
215 samples was maintained at 23°C by immersing the 1/16" stainless steel inlet tubing inside a
216 water bath. Gases were extracted through a semi-permeable silicone membrane connected to a
217 vacuum system, and passed through a liquid nitrogen U-tube bath to extract water vapor before
218 entering a quadruple mass spectrometer (Peiffer HiCube).

219 Net Community Production (NCP) was calculated using two methods as described in *Hamme*
220 *et al*., [2012]. The more traditional approach assumes that the water-column is in steady state
221 and that vertical and lateral mixing are negligible. Therefore the net biological production or
222 consumption of O_2 in the mixed layer can be estimated from the gas-exchange of biological O_2
223 [*Kaiser et al.*, 2005] as:

(1) $$NCP = k_w * O_2eq * \Delta(O_2/Ar)$$

224 where k_w is the weighted gas transfer velocity for O_2 (m d^{-1}), O_2eq is the equilibrium
225 concentration of dissolved O_2 (mmol m^{-3}) in the mixed layer, and $\Delta(O_2/Ar)$ is the deviation of
226 O_2/Ar from equilibrium, calculated as:

(2) $$\Delta(O_2/Ar) = \left[\frac{(O_2/Ar)_{sample}}{(O_2/Ar)_{sat}} - 1\right]$$

227 where $(O_2/Ar)_{sample}$ is the measured ratio in the sample, and $(O_2/Ar)_{sat}$ is the ratio expected at
228 saturation equilibrium, calculated using the solubility equations of *Garcia and Gordon* [1992]
229 for O_2 and *Hamme and Emerson* [2004] for Ar. The gas transfer velocity used in equation (1)

was estimated from the wind speeds recorded at the WHOTS buoy using the wind-speed parameterization and Schmidt numbers from *Wanninkhof* [2014] and a 20-day weighting algorithm following *Reuer et al*. [2007] to account for wind speed variability prior to the measurement (Table S1). We refer to NCP derived from equation 1 as 'prior O_2/Ar-NCP' as it averages over a time period prior to the measurements. An alternative approach to calculate NCP is from the rate of change of $\Delta(O_2/Ar)$ during the expedition by fitting a linear regression to $\Delta(O_2/Ar)$ with time [*Hamme et al.*, 2012].

$$(3) \quad NCP = k_{O2} * O_2eq * \Delta(O_2/Ar) + MLD \frac{d(\Delta(O_2/Ar))}{dt} * O_2eq$$

where k_{O2} is the non-weighted gas transfer velocity for O_2, *MLD* is the average mixed layer depth, and the rate of change of $\Delta(O_2/Ar)$ was calculated by fitting a linear regression to the daily $\Delta(O_2/Ar)$ values. This method has previously been reported for NCP over timescales of hours to days [*Hamme et al*., 2012; *Tortell et al*., 2014] and is hereafter referred to as 'real-time O_2/Ar-NCP', as it averages over the period of time when the measurements were taken.

Samples for triple O_2 isotope ($^{17}\Delta$) analysis were collected during the third major expedition. Measurements were made daily from a depth of 25 m at 0800 hrs from 23 August to 7 September and also at 4 h intervals between 31 August and 1 September. The same sampling and analytical protocols were followed as reported by *Juranek and Quay* [2005]. Samples were collected from Niskin bottles into pre-evacuated, $HgCl_2$ poisoned, 200 mL glass flasks to limit atmospheric contamination. Samples were analyzed at Oregon State University using the same mass spectrometer measurement procedure as described in *Juranek and Quay* [2005]. Rates of gross primary production ($^{17}\Delta$-GPP) were determined as per the method of *Luz and Barkan* [2000] using the water-column parameters, MLD, wind speeds, and gas transfer velocity as described for determining NCP from O_2/Ar analysis [Table S1].

252 A comparison of the four productivity measurements is provided in Table 2 based on MLD-
253 integrated production in units of O_2. The volumetric rates of ^{14}C-PP and FRRF-PP were
254 converted to MLD-integrated values assuming the 25 m sampling depth was representative of the
255 mixed layer. The ^{14}C-PP measurements were converted to equivalent units of O_2 using a
256 photosynthetic quotient (PQ) of 1.1 which is suitable for regenerated production in the
257 oligotrophic gyre ecosystem [*Laws*, 1991]. To identify differences between rates of production
258 for the separate expeditions a two-way analysis of variance (two-way ANOVA) and two-sample
259 t-test was utilized after checking data for heterogeneity of variance.
260
261 *2.3 Additional datasets used*
262 The online Global Marine Argo Atlas dataset was used to help analyze Argo float datasets
263 for sea-surface salinity in the vicinity of Stn ALOHA during July-September 2012 [*Roemmich*
264 *and Gilson*, 2009]. In particular, vertical profiles of pressure, temperature, and conductivity
265 were retrieved from three Webb Research APEX profiling floats (Float IDs #5903888, 5903273,
266 5902241) that were in the vicinity of Stn ALOHA during July-September 2012. The profiles
267 were conducted between the surface and 1000 m every 2-, 5-, and 10-day intervals for the three
268 floats, respectively.
269 Meteorological measurements were provided by the WHOTS buoy situated at Stn ALOHA
270 from June 2012 to July 2013 (http://uop.whoi.edu/projects/WHOTS/whotsdata.htm).
271 Downwelling irradiance above the sea-surface in the PAR spectral region was measured using a
272 cosine sensor (LI-COR LI-192) mounted on the top deck of the R/V Kilo Moana. Measurements
273 of horizontal velocity in the upper water column were obtained using a hull-mounted Acoustic
274 Doppler Current Profiler (ADCP) (RDI Ocean Surveyor 300-kHz). To place the shipboard

measurements in a wider spatial-temporal context, the surface flow within the Hawaii regional domain (15–27°N, 150–160°W) was analyzed using the Hybrid Coordinate Ocean Model (HYCOM) which is run in real-time at the Naval Oceanographic Office at 1/12 degree resolution [*Chassignet et al*., 2009]. Satellite observations of regional ocean color (2002-2012, 8 day averages) for the NPSG were analyzed using images from Moderate Resolution Imaging Spectroradiometer (MODIS) obtained from the Ocean Biology Processing Group (OBPG; http://oceancolor.nasa.gov). Data for a 25x25 km region surrounding Station ALOHA were binned to generate the average and standard deviation at 8-day intervals (e.g. mean of day 1-8 over 2002-2012). Monthly composites were generated for the North Pacific. Anomaly time-series were calculated by difference of 2012 data relative to spatial or temporal averages. Sea Surface Height Anomaly (SSHA) was assessed using animations of satellite altimetry covering 15–30°N 148–170°W and produced from Archiving, Validation, and Interpretation of Satellite Oceanographic data (AVISO).

3. Results

3.1 Hydrographic conditions

During July-September 2012 hydrographic conditions in the upper water-column (0–200 m) showed both the expected seasonal characteristics of the oligotrophic gyre ecosystem based on the 1989-2011 climatology at Stn ALOHA and evidence of high day-to-day variability (Figure 1). At the beginning of the field campaign, during 10-20 July, the mean near-surface (0–25 m) seawater temperature was 24.7 ± 0.1 (standard deviation; SD) °C (Figure 1a). During the following 5 weeks from 20 July to 28 August the 0–25 m seawater temperature increased steadily to a maximum of 25.6°C and then subsequently decreased during the remainder of the

298 campaign (Figure 1b-e). For the overall period during July-September 2012, the near-surface
299 (0–25 m) seawater temperature was 0.7–0.9°C lower than the respective monthly averages from
300 the 1989–2011 climatology at Stn ALOHA, reflecting a long-term interannual anomaly. The
301 near-surface salinity ranged from 35.1–35.4 between July and mid-August 2012 (Figure 1f-i).
302 However initially during 17–18 August and then more consistently from 26 August onwards,
303 salinity decreased coincident with the passage of an upper ocean salinity minimum feature at Stn
304 ALOHA. The mean salinity of the near-surface ocean during 17–18 August was 35.0 and from 6
305 September onwards was 35.0 which represented a mean decrease of 0.3 compared to the salinity
306 measured during July 2012 (Figure 1f-i). The feature was restricted to the near-surface of the
307 water-column with salinity increasing to ~35.2 by a depth of 50 m. Dissolved O_2 concentrations
308 in 0–25 m of the water-column ranged from 209–218 μmol kg^{-1} (represented by the 5 and 95
309 percentile, respectively) with an overall mean of 212 ± 0.1 (SD) μmol kg^{-1} (Figure 1k-o).
310 Between depths of 50–100 m, a subsurface O_2 maximum was present with mean O_2
311 concentrations of 220 ± 3 (SD) μmol kg^{-1}. The deep chlorophyll maximum (DCM) was
312 consistently present at depths between 100–150 m (Figure 1p-t).
313 The mean MLD during 8–20 July 2012 was 66 ± 13 (SD) m, with a maximum depth of 86 m
314 (Figure 1). For the remainder of the study period (20 July to 9 September) the MLD was
315 shallower, with a mean depth of 51 ± 12 (SD) m. The prolonged period of deeper mixing in
316 early July is unusual for the period of July-September at Stn ALOHA (the mean depth based on
317 the 1988-2011 climatology is 49 ± 11 (SD) m). Shipboard observations at Stn ALOHA between
318 1989 and 2011 reveal five occurrences when the cruise-averaged-MLD exceeded 60 m during
319 June-September based on a potential density anomaly of 0.125.

Satellite derived SSHA in the ALOHA region between July and September 2012 suggested relatively modest eddy activity, with SSHA varying between -3.09 cm and 8.53 cm. The largest excursions in SSHA occurred in early July and September due to the westward advection of eddies approximately 180 km to the north of Stn ALOHA.

3.2 Sea-surface salinity minimum at Stn ALOHA in August-September 2012

In addition to the shipboard CTD measurements (Figure 1), vertical profiles of salinity, temperature, and O_2 were collected by Seagliders (Figure 2) and Argo floats (Figure 3). These *in situ* observations provided an estimate of the temporal extent of the sea-surface salinity minimum feature observed in August-September (Figure 1f). The Seaglider traversed an area approximately 2500 km^2 in size and the sea-surface salinity minimum feature was observed at Stn ALOHA until late September (0–25 m mean ± SD salinity of 35.1 ± 0.2), after which time salinity in the near-surface ocean returned to values more typical of late summer and early fall based on the HOT program climatology. Argo floats also detected the sea-surface salinity minimum both in September and prior to its arrival at Stn ALOHA in August (Figure 3). The sea-surface salinity minimum was most evident in the salinity profiles recorded by Argo float #5903888 (0–25 m depth-averaged salinity mean ± SD of 35.0 ± 0.03 during 12 September to 7 October), which profiled at 2 day intervals and was drifting clockwise around Stn ALOHA during July to December 2012 (Figure 3a). The two other Argo floats were located 200-300 km south-east of Stn ALOHA and recorded mean 0–25 m depth-averaged salinity of 35.0 ± 0.1 (SD) during 11 June and 25 September (Float #5903273; Figure 3b) and 35.0 ± 0.1 (SD) during 7 July and 25 September (Float #5902241; Figure 3c). Similar to the Seaglider, the three Argo floats did not continue to detect the sea-surface salinity minimum in October indicating that it had

dissipated or propagated elsewhere undetected. Analysis of the Argo float data to the west and north of Stn ALOHA during September to December 2012 did not reveal any surface salinity minimum features. It is also noteworthy that neither the Argo floats or the Seaglider detected the sea-surface salinity minimum on 17–18 August when it was sampled by the shipboard CTD, indicating the feature was initially irregular and hard to detect.

Efforts to determine the size and origin of the sea-surface salinity minimum proved difficult since it was not evident in satellite-derived measurements of salinity and there were no changes in SSHA associated with the sea-surface salinity minimum. Analysis of circulation patterns generated by the HYCOM model revealed a mean sea-surface flow from the south-east during August to September 2012 (data not shown) and Argo-derived salinity profiles indicated decreased near-surface salinity south-east of Stn ALOHA prior to September 2012 (Figure 3d-e). Using the Argo float monthly-averaged 0–100 m salinity during 2004–2014 for September, a northwest latitudinal shift of the mean salinity field by ~500 km would bring seawater with salinity of 35.0 to Stn ALOHA.

3.3 Water-column particulate material and nutrients

Water-column nutrients and particulate material were sampled at 3 day intervals or greater between depths of 0–175 m during July-September 2012. Depth-averaged (5–25 m) phosphate concentrations ranged from 0.07–0.14 μmol L^{-1} during July-September 2012 (Figure 4a). The phosphate concentrations during July-September are consistent with the 5–25 m depth-averaged values observed throughout 2012 (mean ± SD of 0.1 ± 0.02 μmol L^{-1}); however, the phosphate concentrations in 2012 are high compared to the overall mean of 0.06 ± 0.03 (SD) μmol L^{-1} for 1989-2011 climatological record. Hence the elevated concentrations of phosphate in 2012

366 appear indicative of interannual variability, rather than short-term (monthly) variability.
367 Concentrations of NO_2^- + NO_3^- (not shown in Figure 4) were consistently low in the near-surface
368 water-column during July-September 2012. An increase in NO_2^- + NO_3^- concentrations to 6–8
369 nmol L^{-1} (5–25 m depth-averaged) was recorded by the HOT program during July-August
370 (http://hahana.soest.hawaii.edu/hot/hot-dogs), but not captured during the longer C-MORE
371 expeditions which reported consistently low (2–5 nmol L^{-1}) concentrations.
372 During the period of study, the mean depth-averaged (5–25 m) concentration of PC was 2.3 ±
373 0.3 (SD) µmol L^{-1} (Figure 4b). The most distinct trend was observed during August-September
374 as a persistent decrease in PC concentrations associated with the sea-surface salinity minimum.
375 The lowest PC concentration of 1.7 ± 0.01 µmol L^{-1} was observed on 5 September. This is at the
376 lower end of the long-term PC concentrations at Stn ALOHA for July-September, which range
377 from 1.1–3.8 µmol L^{-1} (mean ± SD of 2.3 ± 0.5 µmol L^{-1}) based on the 1989-2011 HOT
378 climatology. In comparison, the mean 5–25 m depth-averaged concentration of PN for July-
379 September was 0.32 ± 0.06 (SD) µmol L^{-1} (Figure 4c). A similar decreasing trend was observed
380 in PN concentrations compared to PC toward the end of the campaign with the lowest PN
381 concentration (0.24 µmol L^{-1}) measured on 5 September 2012 (Figure 4c).
382
383 *3.4 Phytoplankton community composition*
384 The abundance of flow cytometry-enumerated populations of phytoplankton and
385 heterotrophic picoplankton (bacteria and archaea) in the upper water-column showed a coherent
386 and collective spatial and temporal pattern during July-September 2012 (Figure 5). The 5–25 m
387 depth-averaged mean abundance of *Prochlorococcus* during the overall period from July-
388 September was 1.6 ± 0.3 (SD) x 10^5 cells mL^{-1}. An approximate 17% decrease in 5–25 m depth-

averaged mean cell abundance was observed during 1–7 September (1.4 ± 0.3 (mean ± SD) x 10^5 cells mL^{-1}), coincident with the presence of the sea-surface salinity minimum (Figure 5a-c). Variability was also evident in the vertical distribution of *Prochlorococcus* with maximum cell abundances occurred at 75 m where concentrations averaged 2.1 ± 0.3 (mean ± SD) x 10^5 cells mL^{-1} during July-September. The abundance of *Prochlorococcus* decreased rapidly with depth below 75 m and cell concentrations were ~25% of the maximum abundance at 125 m. *Synechococcus* abundance at 5–25 m depths was 2 orders of magnitude lower than *Prochlorococcus* during July-September, with a mean abundance of 1.2 ± 0.4 (SD) x 10^3 cells mL^{-1} (Figure 5). Similar to the temporal patterns of *Prochlorococcus,* the population of *Synechococcus* also decreased during 1–7 September by ~28% with a mean cell abundance of 0.8 ± 0.1 (SD) x 10^3 cells mL^{-1} (Figure 5). The mean abundance of photosynthetic picoeukaryotes between 5–25 m was 0.9 ± 0.3 (SD) x 10^3 cells mL^{-1} during July-September (Figure 5j-l) and the mean abundance of free-living heterotrophic picoplankton was 5.2 ± 0.7 (SD) x 10^5 cells mL^{-1} (Figure 5d-e). The effect of the sea-surface salinity minimum was also evident in populations of photosynthetic picoeukaryotes and heterotrophic picoplankton which were 33 and 24 % less abundant between depths of 5–25 m during 1–7 September compared to July-August 2012.

In addition to flow cytometry enumerations of cell abundance, phytoplankton pigments at the 25 m depth horizon were sampled at daily (or more frequent) intervals, in addition to vertical profiles every 3 days (Figure 6). The most abundant pigments analyzed were zeaxanthin (Figure 6a), divinylchlorophyll *a* (Figure 6b), and monovinylchlorophyll *a* (Figure 6c). Divinylchlorophyll *a*, the diagnostic pigment for *Prochlorococcus*, was significantly lower in concentration during 7–14 August with a mean concentration of 31 ± 4 (SD) ng L^{-1} compared to 7–23 July (mean ±

412 SD: 46 ± 10 ng L^{-1}) and 23 August to 10 September (mean ± SD: 51 ± 7 ng L^{-1}) (Figure 6b).
413 Daily excursions in pigment concentrations were occasionally observed (*e.g.* 31 August) and
414 coincided with small-scale patterns in local hydrography (Figure 1). Of the three lesser abundant
415 pigments, 19′-hexanoyloxyfucoxanthin and fucoxanthin, diagnostic biomarkers for
416 prymnesiophytes and diatoms respectively, displayed the largest variability during July-
417 September 2012 (Figure 6d, 6e). The highest concentrations of fucoxanthin were observed in
418 July (mean ± SD: 6 ± 1 ng L^{-1}) with concentrations subsequently decreasing steadily throughout
419 the summer (Figure 6e).
420 Depth-averaged (5–25 m) concentrations of *nifH* gene copies for four major groups of N_2
421 fixing microorganisms are shown in Figure 7. UCYN-A, was the most prominent diazotroph
422 during July-September 2012 with an overall mean abundance of 6.8 ± 5.0 (SD) x 10^5 *nifH* gene
423 copies L^{-1}. *Trichodesmium* increased in abundance during the summer to reach a maximum gene
424 abundance of 4.4 x 10^4 *nifH* gene copies L^{-1} during late August-September. The heterocystous
425 cyanobacteria were most abundant in July with a mean concentration of 7.1 ± 1.5 (SD) x 10^3
426 *nifH* gene copies L^{-1} and subsequently decreased in abundance during the summer.
427 *Crocosphaera* was detected throughout July-September with a mean gene abundance of 6.4 ± 3.4
428 (SD) x 10^3 *nifH* gene copies L^{-1}.
429
430 *3.5 Productivity measurements*
431 Measurements of O_2/Ar ratios and ^{14}C assimilation were conducted during all three major
432 expeditions, while FFRF and $^{17}\Delta$ were limited to fewer measurements (Figure 8; Table 2). The
433 O_2/Ar measurements are represented by ΔO_2/Ar(%) including the linear regressions used to
434 calculate real-time O_2/Ar-NCP (Figure 8a) and prior O_2/Ar-NCP in units of mmol O_2 m^{-2} d^{-1}

435 (Figure 8b). Rates of prior O_2/Ar-NCP were significantly different (t-test, $P<0.01$) for each of
436 the major expeditions and demonstrated a clear change between net autotrophic and net
437 heterotrophic conditions in the near-surface waters (Figure 8a, Figure 8b). During 9–24 July, the
438 mean prior O_2/Ar-NCP was 6.0 ± 3.2 (SD) mmol O_2 m^{-2} d^{-1} while the real-time O_2/Ar-NCP was
439 1.6 ± 2.6 (SD) mmol O_2 m^{-2} d^{-1}. The decrease in O_2/Ar-NCP during July ultimately led to net
440 heterotrophic conditions being present in the mixed layer by the time daily measurements were
441 resumed on 5 August. During 5–12 August, the mean MLD-integrated prior O_2/Ar-NCP was -
442 7.6 ± 4.2 (SD) mmol O_2 m^{-2} d^{-1} while real-time O_2/Ar-NCP was positive 3.9 ± 2.2 (SD) mmol O_2
443 m^{-2} d^{-1}, indicating the ecosystem had either recovered from the period of net heterotrophy or
444 there was spatial variability in ΔO_2/Ar. While temporal trends on weekly timescales were
445 present in rates of real-time O_2/Ar-NCP during 8–24 July and 5–12 August (Figure 8a), this was
446 not the case for 22 August to 5 September (Figure 8a). In the absence of temporal trends of
447 weekly timescales, O_2/Ar measurements during 23 August to 6 September were characterized by
448 high day-to-day variability with a mean MLD-integrated prior O_2/Ar-NCP was -0.5 ± 3.1 (SD)
449 mmol O_2 m^{-2} d^{-1}. The variability in prior O_2/Ar-NCP both pre-empted and coincided with the
450 arrival of the sea-surface salinity minimum feature and therefore was likely due to high spatial
451 variability.

452 Rates of ^{14}C-PP sampled at 25 m during every major expedition similarly revealed distinct
453 patterns during July-September 2012 (Figure 8c). The highest rates of ^{14}C-PP occurred during
454 9–25 July with a mean of 0.61 ± 0.1 (SD) mmol C m^{-3} d^{-1} (MLD-integrated 36.3 ± 6.5 mmol C
455 m^{-2} d^{-1}). The lowest rates occurred during 6–12 August with a mean value of 0.49 ± 0.1 (SD)
456 mmol C m^{-3} d^{-1} (MLD-integrated 26.7 ± 5.1 mmol C m^{-2} d^{-1}). During 23 August to 8
457 September, the rates of ^{14}C assimilation ranged from 0.48–0.72 mg C m^{-3} d^{-1}, with an overall

458 mean of 0.62 ± 0.1 (SD) mmol C m^3 d^{-1} (MLD-integrated 33.1 ± 7.4 mmol C m^{-2} d^{-1}). A
459 comparison of the three expeditions revealed significantly lower rates of ^{14}C assimilation during
460 7–14 August (t-test, $P<0.001$), however there was no significant difference between the ^{14}C
461 assimilation rates during 9–25 July and 23 August to 7 September (t-test, $P>0.05$; Table 2).
462 The FRRF-based measurements of productivity (FRRF-PP) were conducted during 9–25 July
463 and 23 August to 8 September (Figure 8d). There was no significant difference (t-test, $P>0.05$)
464 between the mean values of FRRF-PP measured at a depth of 25 m during the two expeditions
465 which were 0.66 ± 0.13 (SD) mmol C m^{-3} d^{-1} for 9–25 July and 0.72 ± 0.07 (SD) mmol C m^{-3} d^{-1}
466 for 23 August to 8 September. A consistent downward trend in FRRF-PP was observed during
467 23 August to 4 September which coincided with the decreasing concentrations of PC (Figure 4).
468 The values of FRRF-PP are provided in Table 2 as MLD-integrated rates of production, using the
469 MLD values provided in the supporting information.
470 Measurements of dissolved triple O_2 isotopes to determine GPP ($^{17}\Delta$-GPP) were conducted
471 on 22 separate occasions during 23 August to 7 September (Table S2). The mean MLD-
472 integrated $^{17}\Delta$-GPP for the 12 day period was 91 ± 35 (SD) mmol O_2 m^{-2} d^{-1} (range of 38–168
473 mmol O_2 m^{-2} d^{-1}). The analysis of duplicate seawater samples on the 28 August yielded a mean ±
474 SD of 51 ± 5 mmol O_2 m^{-2} d^{-1} (Table S2). The $^{17}\Delta$-GPP was almost 3-fold higher than MLD-
475 integrated ^{14}C-PP and 40% higher than MLD-integrated FRRF-PP during 23 August to 7
476 September (Table 2).
477 The significant period of low productivity when the upper water-column was in a net
478 heterotrophic state was explored using other datasets including phytoplankton biomarkers, time-
479 series climatological measurements, and satellite-derived TChl*a*. During 7–12 August, the low
480 rates of productivity coincided with low concentrations of TChl*a*, an indicator of photosynthetic

biomass (Figure 8e). The mean concentration of TChl*a* decreased at the 25 m depth horizon from 82 ± 6 (SD) ng L^{-1} in 9–25 July by 30% to 66 ± 6 (SD) ng L^{-1} in 6–13 August (Figure 8e). The mean concentration of TChl*a* subsequently increased to an average concentration of 82 ± 7 (SD) ng L^{-1} for 23 August to 7 September (Figure 8e). A comparison of the three expeditions revealed significantly lower concentration of TChl*a* during 7–12 August (t-test, $P<0.001$), however there was no significance difference between concentration of TChl*a* during 9–25 July and 23 August to 7 September (t-test, $P>0.05$).

The HOT program's near-monthly measurements at Stn ALOHA of ^{14}C assimilation and particle export rates during March-October 2012 are shown in comparison with the 1989-2011 HOT climatology (Figure 9). The monthly time-series measurements support the observation of low productivity occurring during August 2012. The mean depth-averaged (5–25 m) rates of ^{14}C-PP rates measured on 17 August was 0.44 mmol C m^3 d^{-1} (Figure 9a), equivalent to a MLD-integrated rate of ^{14}C-PP of 20.6 mmol C m^{-2} d^{-1}. These rates of ^{14}C-PP are low for this time of year at Stn ALOHA with a monthly mean for August based on the 1989-2011 HOT climatology of 0.66 ± 0.2 mmol C m^{-3} d^{-1} (Figure 9a). In addition to ^{14}C assimilation, during 17–18 August 2012, measured downward export of C was 1.5 mmol C m^{-2} d^{-1}, almost half of the the mean ± SD (2.9 ± 0.9 mmol C m^{-2} d^{-1}) for the month of August during the 1989-2011 Stn ALOHA climatology (Figure 9b).

The spatial and temporal extent for the period of low productivity was further investigated using remote sensing products provided by MODIS. Satellite-derived TChl*a* concentrations for 2012 are compared with the antecedent 10-year climatology (Figure 9c). The period of low productivity observed during 4–14 August by shipboard measurements is accompanied by a decrease in satellite-derived TChl*a* relative to the 10-year mean. However there is a temporal

mis-match with the shipboard measurements of TChl*a*, as determined by HPLC and fluorometry, as the satellite data shows the largest TChl*a* anomaly to be in September 2012 when concentrations of TChl*a* are less than the minimum values observed in the 10-year climatology. In contrast, the shipboard observations show August to have the lowest TChl*a* concentrations (Figure 8e). A broader look at the TChl*a* anomaly throughout the NPSG reveals the negative anomaly is evident in August-September, but not earlier in July 2012 (Figure 10). Albeit patchy, the negative TChl*a* anomaly during August-September extended from 22–26°N to 152–160°W, a region of approximately 300,000 km^2.

4. Discussion

4.1Insights from high-resolution sampling in July-September 2012

The NPSG is a characteristic oligotrophic ecosystem with warm, stable conditions aided by strong seasonal stratification. Time-series observations conducted by the HOT program at Stn ALOHA for nearly three decades have characterized the frequently subtle seasonal and interannual variability associated with key physical and biological processes. For example, 0–200 m depth-integrated rates of primary productivity as determined by ^{14}C assimilation during 1988–2012 are 1.5 times higher in June-August (mean ± SD: 50.7 ± 11.8 mmol C m^{-2} d^{-1}) compared to December-February (mean ± SD: 34.7 ± 8.5 mmol C m^{-2} d^{-1}). One of the benefits of the long-term time-series observations is the ability to report the monthly or seasonal variability throughout several decades and the mean rate of ^{14}C assimilation in the month of August is 52.6 ± 11.1 (SD) mmol C m^{-2} d^{-1}, ranging from 39.8–68.8 mmol C m^{-2} d^{-1} (represented by the 5 and 95 percentile values). This highlights that the variability within a single month can almost equal the variability measured within an entire annual period, suggesting that the short-

term phenomena (*e.g*. phytoplankton blooms, mesoscale eddies, and wind-driven mixing) play an important role in shaping elemental cycling and phytoplankton growth. Until now however, high-resolution analysis of a single seasonal period using intensive shipboard time-series measurements has not been conducted alongside the HOT program.

During July-September 2012, high temporal-resolution sampling at Stn ALOHA revealed changes in water-column biogeochemical properties over time-scales of days to weeks. Overall, the measurements recorded a period of anomalously low productivity with a prolonged event of net heterotrophy in the upper water-column. Our observation coincided with an absence of mesoscale eddies, a near-ubiquitous feature of the NPSG which advect through Stn ALOHA. While the focus of this study was on the upper ocean productivity and community composition (*Section 4.2*), an analysis of the longer-term temporal variability and the wider NPSG is required to contextualize the findings from July-September 2012 (*Section 4.3*).

4.2 Productivity and community structure in July-September 2012

An overall picture of NCP at Stn ALOHA between July-September 2012 is provided by the daily measurements of O_2/Ar ratio. Positive rates of NCP were initially measured in early July, but began to decrease until ultimately net heterotrophic conditions were recorded in early August. It is unfortunate that the transition period occurred in-between the two expeditions, although noteworthy that the changes occurred over timescales of several weeks. Overall it is unusual for such a prolonged period of net heterotrophy to be present during the summer at Station ALOHA [*Emerson et al.*, 1997; *Juranek and Quay*, 2005; *Quay et al*., 2010]. The magnitude of the low productivity is apparent when comparing prior O_2/Ar-NCP measured during 6–12 August in units of O_2 (-7.6 ± 4.2 mmol O_2 m^{-2} d^{-1}) with the summary of NCP

550 measurements previously reported for Stn ALOHA based on *in situ* geochemical methods (range
551 from 3–11 mmol O_2 m^{-2} d^{-1}) [*Williams et al*., 2013 and references therein]. The mixed layer
552 community subsequently recovered from the period of net heterotrophy although rates of NCP
553 were still comparatively low during 22 August to 6 September which was attributed to the sea-
554 surface salinity minimum. The three cruises are examined chronologically with regards to
555 productivity and biological community composition.
556 During July the mixed layer depth became progressively more shallow (Figure 1) and from
557 20 July onwards (for the next 5 weeks) the near-surface seawater (0–25 m) temperature increased
558 by 1°C. During 7–23 July, ΔO_2/Ar values were at their maximum recorded during July-
559 September and the mean MLD-integrated prior O_2/Ar-NCP was 6.0 ± 3.2 (SD) mmol O_2 m^{-2} d^{-1}.
560 During this period, although the ΔO_2/Ar values were positive, indicating recent net autotrophic
561 production, there was a decrease in ΔO_2/Ar values with time, indicating that either the system
562 was not in steady state, or there was some spatial variability in ΔO_2/Ar. Estimated real-time
563 O_2/Ar-NCP for this period was 1.6 ± 2.6 (SD) mmol O_2 m^{-2} d^{-1}, four times lower than the mean
564 prior O_2/Ar-NCP. During this period, concentrations of fucoxanthin, the diagnostic pigment
565 biomarker for diatoms were at their summer maximum with a mean of 5.7 ± 1.1 (SD) ng L^{-1}
566 (Figure 6e). Furthermore, the combined total *nifH* gene copies for heterocystous cyanobacteria
567 were also at their maximum with an average abundance of 7.1 ± 1.5 (SD) x 10^3 gene copies L^{-1}
568 during 10–24 July (Figure 7). We therefore infer that the positive NCP during July was driven
569 by diatoms that host symbiotic diazotroph assemblages. The identity of the heterocystous
570 cyanobacteria determined by gene analysis was the endosymbiont *Richelia intracellularis* which
571 is associated with the diatoms *Rhizosolenia* and *Hemiaulus* [*Foster and O'Mullan*, 2008]. High
572 abundances of diatom-diazotroph assemblages have been associated with major increases in

surface TChl*a* concentration [*Wilson*, 2003; *Fong et al*., 2008; *Villareal et al*., 2012] and the seasonal pulse of exported material that occurs at Stn ALOHA each year between July and August is thought to be fueled by these symbiotic micro-organisms [*Karl et al*., 2012]. A separate study on particle distributions in the euphotic zone at Stn ALOHA during July-September 2012 showed a positive correlation ($R^2 = 0.24$, $p<0.05$) between fucoxanthin concentrations and 20-100 µm sized particles [Barone *et al*., 2015]. Both fucoxanthin and 20-100 µm sized particles have the highest concentrations and the largest variability during July and are most likely the cause of the higher variability observed in the FRRF-derived estimates of productivity during July compared to the 22 August to 11 September expedition (Figure 8d).

By the start of the second leg of the three C-MORE expeditions (4–14 August), the pattern of NCP had changed. $\Delta O_2/Ar$ values were negative, indicating a recent period of net heterotrophy and prior-O_2/Ar-NCP values were also negative with a mean value of -7.6 ± 4.2 mmol O_2 m^{-2} d^{-1}. However, $\Delta O_2/Ar$ values during this period showed an increase with time and therefore real-time O_2/Ar-NCP was positive, with a mean value of 3.9 ± 2.2 mmol O_2 m^{-2} d^{-1}. Again, this indicates that either the mixed layer was recovering from the period of net heterotrophy or there was spatial variability in $\Delta O_2/Ar$. The mismatch between prior and real time NCP has been previously observed [*Hamme et al.*, 2012], whereas in other occasions both approaches agree well [*Ferrón et al.*, 2015]. Rates of ^{14}C-PP are lowest during 6–12 August (mean ± SD: 26.7 ± 5.1 mmol C m^{-2} d^{-1}) and remained low until 18 August when *in situ* ^{14}C measurements were conducted by the HOT program (Figure 9). The low productivity period was accompanied by a decrease in concentrations of photosynthetic pigments TChl*a* (Figure 8e), Zeax, and dvchl*a* (Figure 6a and 6b), indicating an accompanying shift in the dominant phytoplankton population. Despite changes in productivity and community composition, there was low variability in the

596 hydrographic structure of the water-column or nutrient conditions to accompany the rapid change
597 from net autotrophic to net heterotrophic conditions. During 23 August to 7 September,
598 measurements of ^{14}C-PP and O_2/Ar-NCP were accompanied by measurements of FRRF-PP and
599 $^{17}\Delta$-GPP. Simultaneous measurements of the four methods of productivity are infrequently
600 achieved, particularly for a 15-day period in the open ocean, and therefore offer an insight into
601 the daily variability of these parameters when there was high spatial heterogeneity in the upper
602 water-column. While MLD-integrated prior O_2/Ar-NCP remained low for this period with a
603 mean of -0.5 ± 3.1 (SD) mmol O_2 m^{-2} d^{-1}, rates of ^{14}C-PP had increased from the low values
604 measured during 6–12 August to a mean of 33.1 ± 7.4 (SD) mmol C m^{-2} d^{-1}. Overall MLD-
605 integrated $^{17}\Delta$-GPP averaged 90.7 ± 35.3 mmol O_2 m^{-2} d^{-1} for the entire 15 day period and were
606 comparable with previous measurements at Stn ALOHA in the summertime [*Juranek and Quay,*
607 2005; *Quay et al.*, 2010]. The high variability in the MLD-integrated $^{17}\Delta$-GPP measurements is
608 supportive of the observation that there was high lateral heterogeneity in the surface seawater
609 during this period. The O_2-based productivity estimates extrapolate for the residence time of O_2
610 in the mixed layer which sets a boundary on how much they can vary over a 24 h period.
611 Considerable day-to-day variability was also observed in the O_2/Ar measurements with one of
612 the largest decreases in prior O_2/Ar-NCP on 4 September when the near-surface water column
613 became undersaturated (99.7%) in dissolved O_2 (Table S1). This coincided with a strong
614 decrease in salinity associated with the sea-surface salinity minimum (Figure 1). The most
615 consistent temporal trend in the different measurements of productivity was evident in FRRF-
616 derived estimates which decreased continually during the observation period. FRRF-PP is
617 considered to more closely resemble GPP, however it was ~40% lower than $^{17}\Delta$-GPP during 23
618 August to 7 September 2012. The decrease in FRRF-PP is coincident with decreasing

619 concentrations of flow cytometry-enumerated phytoplankton abundance (Figure 5) and
620 particulate material (Figure 4). Ultimately the overall broad overview from this period is that the
621 near-surface water-column was recovering from a net heterotrophic state although MLD-
622 integrated prior O_2/Ar-NCP are still comparatively low and the sea-surface salinity minimum
623 was accompanied by substantial spatial variability.
624
625 *4.3 Further analysis of the low productivity period*
626 It is unusual to observe an intensive period of net heterotrophic conditions during the summer
627 at Stn ALOHA. The pronounced period of net heterotrophy occurred during the 4–14 August
628 expedition, however prior O_2/Ar-NCP during 26 August to 5 September was still relatively low
629 (-0.5 ± 3.1 mmol O_2 m^{-2} d^{-1}) (Figure 8). Satellite observations revealed that the low productivity
630 was not localized to Stn ALOHA as an extensive low TChl*a* anomaly was evident from August
631 through to September across the geographic area from 22–26°N to 152–160°W (Figure 10). The
632 prolonged period of anomalous TChl*a* as revealed by MODIS (Figure 10) is somewhat
633 contradictory to the shipboard pigment measurements (Figure 8e) where HPLC-derived TChl*a*
634 increased in September relative to 4–14 August. However it does suggest the low productivity
635 was a regional phenomenon lasting for 1–2 months. In the absence of any local or regional
636 physical forcing identified, wider ecosystem controls on productivity at Stn ALOHA are
637 considered below.
638 One possible explanation for the low productivity is micro-nutrient limitation which would
639 account for the build-up of phosphate that was at a higher concentration (0–100 m integrated
640 values of 11.3 mmol m^{-2}) during 2012 than any other year (range from 3.0 mmol m^{-2} in 2003 to
641 10.0 mmol m^{-2} in 1999) since 1988 (http://hahana.soest.hawaii.edu/hot/hot-dogs). The

identification of the limiting micro-nutrient(s) was not investigated experimentally during this field program, however near-surface concentrations of dissolved iron ranged from 0.14–0.87 nmol kg^{-1} (mean 0.31± 0.14 nmol kg^{-1}) throughout the summer and may have been limiting for certain phytoplankton species [*Fitzsimmons et al*., in revision Geochimica et Cosmochimica Acta, 2015]. Another factor that directly influences growth and metabolism of marine plankton is seawater temperature [*Laws et al*., 2000] which had a lower annual mean recording (24.5°C) between depths of 0–50 m during 2012 compared to the previous 12 years (24.6–25.4°C) (http://hahana.soest.hawaii.edu/hot/hot-dogs). However the biogeochemical trends present in August 2012 should also be compared with longer timescales and during the past 5 years (2009–2014), 0–100 m depth-integrated ^{14}C-PP has steadily increased (annual mean of 183 g C m^{-2} d^{-1} in 2009 compared to 233 g C m^{-2} d^{-1} in 2014), while the high phosphate concentrations observed in 2012 subsequently decreased and near-surface seawater temperatures subsequently increased (http://hahana.soest.hawaii.edu/hot/hot-dogs). An additional influence on productivity is near-surface water-column mixing. A 'typical' mixed layer depth during the summertime at Stn ALOHA is 50 m and during 2012 the upper water-column did not stratify to this extent until late July. The ramifications of a delay in stratification on the diazotroph community which have been implicated in bloom formation in the NPSG [*Dore et al*., 2008] are unclear and their abundances during July-September (Figure 7) were at the lower end of their previously reported summertime abundances at Stn ALOHA [*Church et al*., 2009]. Over longer-term timescales, a strengthening in stratification of the upper ocean is generally expected to cause decreased marine primary productivity in the subtropics , although this was not evident from historical analysis of the Stn ALOHA climatology [*Dave and Lozier*, 2010].

4.4 Sea-surface salinity minimum

The hydrographic feature which was uniquely described in this study was a sea-surface salinity minimum restricted to the upper water-column and with biogeochemical properties distinct from the surrounding waters. Although it was difficult to track the source of the sea-surface salinity minimum with any certainty, ADCP and Argo float data indicate that it originated southeast of the Hawaiian Islands. This is supported by analysis of circulation patterns generated by the HYCOM model which revealed that the mean sea-surface flow was from the south-east during August to September 2012. The major ocean current to the southeast of the Hawaiian Islands is the North Equatorial Current, which extends from 10 to 20° N [*Bondur et al*., 2008]. The North Equatorial Current bifurcates to the east of the island of Hawaii and the northern portion then contributes to the North Hawaii Ridge Current (NHRC), a weak predominantly westward flowing current [*Qiu et al*., 1997; *Firing et al*., 1999; *Bondur et al*., 2008]. The magnitude of the NHRC varies considerably, ranging from undetectable to a maximum of 17 cm sec^{-1} with no identified seasonal pattern in magnitude [*Firing*, 1996]. Its northern boundary is usually located south of Stn ALOHA although it was detected intermittently at the time-series monitoring station [*Firing*, 1996].

The sea-surface salinity minimum described in this study provides an important example regarding the effect of discrete features (*e.g*. mesoscale eddy fields, meandering jets, and eddy dipoles) on biogeochemical variability at the ocean surface [*Williams and Follows*, 2011]. These features often have isolated water masses in their interiors for extended periods of time, indicative of transport barriers along their edges [*Harrison and Glatzmeier*, 2010]. For example, the transport of isolated water can provide nutrients into oligotrophic gyres which triggers biological productivity [*e.g*. *Bracco et al*., 2000; *McGillicuddy et al*., 2007]. In this instance

688 there was no evidence for nutrient injection into the oligotrophic ecosystem and instead the
689 dominant effect of the isolation associated with sea-surface salinity minimum was a decline in
690 biomass and productivity.

691 Ultimately, the community structure and biogeochemical signature associated with the sea-
692 surface salinity minimum revealed a decreased microbial abundance which may have resulted
693 from two factors. The first is that its properties are representative of the originating ecosystem
694 remaining unchanged prior to its detection at Stn ALOHA. This is unlikely as a comparison of
695 *Prochlorococcus*, *Synechoccoccus*, and heterotrophic bacteria abundance between Stn ALOHA
696 and the tropical Pacific Ocean (0-10° N, 140° W) do not reveal major abundance differences
697 [*Landry and Kirchman*, 2002]. The second explanation is that biological activity (death, cell
698 lysis, and grazing) caused the decrease in biomass. The cumulative effects of these events would
699 be quite significant (as is the case) due to the isolation of sea-surface salinity minimum from the
700 surrounding water masses. In spite of the decrease in biomass an increase in inorganic nutrient
701 concentrations which might be expected for net remineralization of the organic material was not
702 observed. Most likely the biological material was exported downwards with some retained at the
703 base of the sea-surface salinity minimum (at depths of 50–70 m in the water-column) due to the
704 physical discontinuity resulting from strong stratification.

705 Although the *in situ* autonomous Seagliders and profiling floats were able to measure the
706 extent of the sea-surface salinity minimum which continued through September (Figure 2), it is
707 regrettable that the sampling of the feature was terminated at the end of the campaign. The
708 decreasing concentrations of key water-column properties including particulate material,
709 *Prochlorococcus* abundances, and prior O_2/Ar-NCP suggest that the full extent of the
710 biogeochemical conditions associated with the sea-surface salinity minimum might not have

been evaluated. Increasing deployment of *in situ* sensors to measure O_2 [*Riser and Johnson* 2008], nutrients [*Johnson et al*., 2010], and even community composition and activity [*Robidart et al*., 2014] on autonomous vehicles will help attribute biogeochemical variability to discrete hydrographic features in the future.

5. Conclusion

In an oligotrophic gyre setting, where the ecosystem operates at the interface between net autotrophic to net heterotrophic conditions, our study shows that daily measurements are extremely informative when attempting to characterize intra-seasonal variability and identify its drivers. In some instances changes in plankton community could be related to episodic hydrographic features *e.g*. decrease in cell abundance associated with the presence of the sea-surface salinity minimum. However, in other instances, such as the observed shift from net autotrophic to net heterotrophic conditions between July and August 2012, it is harder to explain the causes. Our inability to separate temporal from spatial variability through our Eulerian sampling approach highlights some of the difficulties faced in the study of pelagic microbial assemblages in which generation scales are in the order of days and kilometers. In the absence of local causation mechanisms being identified, larger spatial-temporal influences were investigated including nutrient concentrations, mixed-layer depth, and seawater temperature. Ultimately extensive ship operations lasting nearly 3 months are difficult to accomplish and advances in obtaining sufficient spatial-temporal resolution will require the integration of autonomous, *in situ* instrumentation including floats, Seagliders, and moorings in collaboration with ship-based observations and experimentation.

Acknowledgements

The dataset presented here resulted from the input of over fifty sea-going and shore-based oceanographers who contributed to the success of the field campaigns in 2012. We thank the Hawaii Ocean Time-series (HOT) program, the R/V *Kilo Moana* captain and crew, L. Fujieki for creating the C-MORE Data System which hosts the C-MORE field data (http://hahana.soest.hawaii.edu/cmoreDS/interface.html), S. Poulos for leading the Seaglider operations (http://hahana.soest.hawaii.edu/seagliders/), and P. Berube, T. Clemente, S. Tozzi for cruise leadership. The WHOTS surface mooring data are provided by R.A. Weller and A. J. Plueddemann (http://www.soest.hawaii.edu/whots/) with funding from the NOAA Climate Observation Division. We thank H. Alexander, D. Böttjer, M. Segura-Noguera, and two anonymous reviewers for critical comments to the manuscript. This research was supported by the National Science Foundation (NSF) Center for Microbial Oceanography: Research and Education (C-MORE) (EF0424599 to D.M.K.), NSF Grant OCE-1153656 (D.M.K) and a Gordon and Betty Moore Foundation Marine Microbiology Investigator award to D.M.K. The HOT program is supported by the NSF (OCE-1260164 to M.J.C, R.R.B., and D.M.K.).

References

Ascani, F., K. J. Richards, E. Firing, S. Grant, K. S. Johnson, K.S., Y. Jia, R. Lukas, and D. M. Karl (2013), Physical and biological controls of nitrate concentrations in the upper subtropical North Pacific Ocean, *Deep Sea Res. Part II, 93*, 119–134, doi:10.1016/j.dsr2.2013.01.034.

Barone, B., R. R. Bidigare, M. J. Church, D. M. Karl, R. M. Letelier, and A. E. White (2015), Particle distributions and dynamics in the euphotic zone of the North Pacific Subtropical Gyre, J. Geophys. Res. Oceans, 120, doi:10.1002/2015JC010774.

Bidigare, R.R., L. Van Heukelem, and C. C. Trees (2005), Analysis of algal pigments by high-performance liquid chromatography, in Algal Culturing Techniques, edited by R. A. Andersen, pp. 327–345, Academic Press, New York, N.Y.

Bidigare, R. R., F. Chai, M. R. Landry, R. Lukas, C. C. S. Hannides, S. J. Christensen, D. M. Karl, L. Shi, and Y. Chao (2009), Subtropical ocean ecosystem structure changes forced by North Pacific climate variations, *J. Plankton Res., 31*, 1131–1139, doi:10.1093/plankt/fbp064.

Bingham, F. M., and R. Lukas (1996), Seasonal cycles of temperature, salinity, and dissolved oxygen observed in the Hawaii Ocean time-series, *Deep Sea Res., Part II, 43*, 199–213, doi:0967-0645(95)00090-9.

Bondur, V. G., R. A. Ibrayev, Yu V. Grebenyuk, and G. A. Sarkisyan (2008), Modeling the sea currents in open basins: The case study for the Hawaiian Island region, *Izvestiya, Atmospheric and Oceanic Physics 44*, 225–235, doi:10.1134/S0001433808020102.

Bracco, A., A. Provenzale, and I. Sheuring (2000), Mesoscale vortices and the paradox of the plankton, *Proc. R. Soc. Lond. B, 267*, 1795–1800, doi 10.1098/rspb.2000.1212.

Carritt, D. E., and J. H. Carpenter (1966), Comparison and evaluation of currently employed modifications of the Winkler method for determining dissolved oxygen in seawater; a NASCO report. *J. Mar. Res. 24*, 286–318.

Chassignet, E. P., H. E. Hurlburt, E. J. Metzger, O. M. Smedstad, J. Cummings, G. R. Halliwell, R. Bleck, R. Baraille, A. J. Wallcraft, C. Lozano, et al. (2009), US GODAE: Global ocean prediction with the HYbrid Coordinate Ocean Model (HYCOM). *Oceanogr. 22*, 64–75 doi: 10.5670/oceanog.2009.39.

Church, M. J., C. Mahaffey, R. M. Letelier, R. Lukas, J. P. Zehr, and D. M. Karl (2009), Physical forcing of nitrogen fixation and diazotroph community structure in the North Pacific subtropical gyre, *Global Biogeochem. Cycles*, 23, GB2020, doi:10.1029/2008GB003418.

Church, M. J., M. W. Lomas, and F. Muller-Karger (2013), Sea change: Charting the course for biogeochemical ocean time-series research in a new millennium, *Deep Sea Res., Part II, 93*, 2–15, doi:10.1016/j.dsr2.2013.01.035.

796 Corno, G., D. M. Karl, M. J. Church, R. M. Letelier, R. Lukas, R. R. Bidigare, and M. R. Abbott
797 (2007), Impact of climate forcing on ecosystem processes in the North Pacific Subtropical Gyre,
798 *J. Geophys. Res., 112*, C04021, doi:10.1029/2006JC003730.
799
800 Dave, A. C., and M. S. Lozier (2010), Local stratification control of marine productivity in the
801 subtropical North Pacific, *J. Geophys. Res., 115*, C12032, doi:10.1029/2010JC006507
802
803 Dore, J. E., and D. M. Karl (1996), Nitrite distributions and dynamics at Station ALOHA, *Deep*
804 *Sea Res., Part II, 43*, 385–402, doi:10.1016/0967-0645(95)00105-0.
805
806 Dore, J. E., R. M. Letelier, M. J. Church, R. Lukas, and D. M. Karl (2008), Summer
807 phytoplankton blooms in the oligotrophic North Pacific Subtropical Gyre: Historical perspective
808 and recent observations, *Prog. Oceanogr., 76*, 2–38, doi:10.1016/j.pocean.2007.10.002.
809
810 Dore, J. E., R. Lukas, D. W. Sadler, M. J. Church, and D. M. Karl (2009), Physical and
811 biogeochemical modulation of ocean acidification in the central North Pacific, *Proc. Natl. Acad.*
812 *Sci. U.S.A., 106*, 12235–12240, doi:10.1073/pnas.0906044106.
813
814 Duarte, C. M., A. Regaudie-de-Gioux, J. M. Arrieta, A. Delgado-Huertas, and S. Agustí (2013),
815 The oligotrophic ocean is heterotrophic, *Annu. Rev. Mar. Sci*., 5, 551–569, doi:
816 10.1146/annurev-marine-121211-172337.
817
818 Emerson, S., P. Quay, D. Karl, C. Winn, L. Tupas, and M. Landry (1997), Experimental
819 determination of the organic carbon flux from open-ocean surface waters, *Nature*, 389, 951-954,
820 doi:910.1038/40111.
821
822 Emerson, S. (2014), Annual net community production and the biological carbon flux in the
823 ocean, *Global Biogeochem. Cycles, 28*, 14–28, doi:10.1002/2013GB004680
824
825 Eriksen, C. C., T. J. Osse, R. D. Light, T. Wen, T. W. Lehman, P. L. Sabin, J. W. Ballard, and A.
826 M. Chiodi (2001), Seaglider: A long-range autonomous underwater vehicle for oceanographic
827 research, *Oceanic Engineering, IEEE J. of, 26*, 424–436, doi:10.1109/48.972073.
828
829 Ferrón, S., S. T. Wilson, S. Martínez-Garcia, P. D. Quay, and D. M. Karl (2015), Metabolic
830 balance in the mixed layer of the oligotrophic North Pacific Ocean from diel changes in O_2/Ar
831 saturation ratios. *Geophys. Res. Lett. 42*, doi:10.1002/2015GL063555.
832
833 Firing, E. (1996), Currents observed north of Oahu during the first five years of HOT, *Deep Sea*
834 *Res., Part II, 43*, 281–303, doi:10.1016/0967-0645(95)00097-6.
835
836 Firing, E., B. Qiu, and W. Miao (1999), Time-dependent island rule and its application to the
837 time-varying North Hawaiian Ridge Current, *J. Phys. Oceanogr., 29*, 2671–2688,
838 doi:10.1175/1520-0485(1999)029<2671:TDIRAI>2.0.CO;2.
839

840 Fong, A. A., D. M. Karl, R. Lukas, R. M. Letelier, J. P. Zehr, and M. J. Church (2008), Nitrogen
841 fixation in an anticyclonic eddy in the oligotrophic North Pacific Ocean, *The ISME J. 2*, 663–
842 676, doi:10.1038/ismej.2008.22.
843
844 Foster, R.A., and G. D. O'Mullan (2008), Nitrogen-fixing and nitrifying symbioses in the
845 marine environment, in Nitrogen in the marine environment , edited by D. G. Capone, D. Bronk,
846 M. Mulholland and E. Carpenter, pp 1197–1218, Elsevier Science, New York.
847
848 Garcia, H. E., and L. I. Gordon (1992), Oxygen solubility in seawater: Better fitting equations,
849 *Limnol. Oceanogr*., *37*, 1307–1312, doi:10.4319/lo.1992.37.6.1307.
850
851 Goebel, N. L., K. A. Turk, K. M. Achilles, R. Paerl, I. Hewson, A. E. Morrison, J. P. Montoya,
852 C. A. Edwards, and J. P. Zehr (2010), Abundance and distribution of major groups of
853 diazotrophic cyanobacteria and their potential contribution to N_2 fixation in the tropical Atlantic
854 Ocean, *Environ. Microbiol*., *12*, 3272–3289, doi:10.1111/j.1462-2920.2010.02303.x.
855
856 Guidi, L., *et al*. (2012), Does eddy-eddy interaction control surface phytoplankton distribution
857 and carbon export in the North Pacific Subtropical Gyre?, *J. Geophys. Res., 117*(G2), G02024,
858 doi:10.1029/2012JG001984.
859
860 Hamme, R. C., and S. R. Emerson (2004), The solubility of neon, nitrogen and argon in distilled
861 water and seawater, *Deep Sea Res., Part I, 51*, 1517–1528, doi:10.1016/j.dsr.2004.06.009.
862
863 Hamme, R. C., N. Cassar, V. P. Lance, R. D. Vaillancourt, M. L. Bender, P. G. Strutton, T. S.
864 Moore, M. D. DeGrandpre, C. S. Sabine, D. T. Ho, and B. R. Hargreaves (2012), Dissolved
865 O_2/Ar and other methods reveal rapid changes in productivity during a Lagrangian experiment in
866 the Southern Ocean, *J. Geophys. Res., 117*, C00F12, doi:10.1029/2011JC007046.
867
868 Harrison, C. S., and G. A. Glatzmaier (2010), Lagrangian coherent structures in the California
869 Current System–sensitivities and limitations, *Geophys. Astrophys. Fluid Dyn., 106*, 22–44, doi:
870 10.1080/03091929.2010.532793.
871
872 Johnson, K. S., S. C. Riser, and D. M. Karl (2010), Nitrate supply from deep to near-surface
873 waters of the North Pacific subtropical gyre, *Nature, 465*, 1062–1065, doi:10.1038/nature09170.
874
875 Juranek, L. W., and P. D. Quay (2005), In vitro and in situ gross primary and net community
876 production in the North Pacific Subtropical Gyre using labeled and natural abundance isotopes of
877 dissolved O_2, *Global Biogeochem. Cycles, 19*, GB3009, doi:3010.1029/2004GB002384.
878
879 Kaiser, J., M. K. Reuer, B. Barnett, and M. L. Bender (2005), Marine productivity estimates
880 from continuous O_2/Ar ratio measurements by membrane inlet mass spectrometry,
881 *Geophys. Res. Lett., 32*, L19605, doi:10.1029/2005GL023459.
882
883 Kana, T. M., C. Darkangelo, M. Duane Hunt, J. B. Oldham, G. E. Bennett, and J. C. Cornwell
884 (1994), Membrane inlet mass spectrometer for rapid high-precision determination of N_2, O_2, and
885 Ar in environmental water samples, *Anal. Chem., 66*, 4166–4170, doi:10.1021/ac00095a009.

Karl, D. M., and R. Lukas (1996), The Hawaii Ocean Time-series (HOT) program: Background, rationale and field implementation, *Deep Sea Res., Part II, 43*, 129–156, doi: 10.1016/0967-0645(96)00005-7.

Karl, D. M., J. E. Dore, D. V. Hebel, and C. Winn (1991), Procedures for particulate carbon, nitrogen, phosphorus and total mass analyses used in the US-JGOFS Hawaii Ocean Time-Series Program, in Marine Particles: Analysis and Characterization, Geophysical Monograph 63, edited by D. W. Spencer and D. C. Hurd, pp. 71–77, American Geophysical Union, Washington DC, USA.

Karl, D. M., R. R. Bidigare, and R. M. Letelier (2002), Sustained and aperiodic variability in organic matter production and phototrophic microbial community structure in the North Pacific subtropical gyre, in: Phytoplankton Productivity and Carbon Assimilation in Marine and Freshwater Ecosystems, edited by P. J. Williams, D. R. Thomas, and C. S. Reynolds, pp. 222–264, Blackwell, Malden, Mass.

Karl, D. M., M. J. Church, R. M. Letelier, and C. Mahaffey (2012), Predictable and efficient carbon sequestration in the North Pacific Ocean supported by symbiotic nitrogen fixation, *Proc. Natl. Acad. Sci. U. S. A.,109*, 1842–1849, doi:10.1073/pnas.1120312109.

Karl, D. M., and M. J. Church (2014), Microbial oceanography and the Hawaii Ocean Time-series programme, *Nat. Reviews Microbiol., 12*, 1–15, doi:10.1038/nrmicro3333.

Keeling, C. D., H. Brix, and N. Gruber (2004), Seasonal and long-term dynamics of the upper ocean carbon cycle at Station ALOHA near Hawaii, *Global Biogeochem. Cycles, 18*, GB4006, doi:10.1029/2004GB002227.

Kolber, Z., and P. G. Falkowski (1993), Use of active fluorescence to estimate phytoplankton photosynthesis *in situ*. *Limnol*. *Oceanogr*., *38*, 1646–1665, doi: 10.4319/lo.1993.38.8.1646.

Landry, M. R., and D. L. Kirchman (2002), Microbial community structure and variability in the tropical Pacific, *Deep Sea Res., Part II, 49*, 2669–2693, doi: 10.1016/S0967-0645(02)00053-X.

Laws, E. A. (1991), Photosynthetic quotients, new production and net community production in the open ocean, *Deep Sea Res., Part I, 38*, 143–167, doi:110.1016/0198-0149(1091)90059-O.

Laws, E. A., P. G. Falkowski, W. O. Smith Jr., H. Ducklow, and J. J. McCarthy (2000), Temperature effects on export production in the open ocean, *Global Biogeochem. Cycles*, *14*(4), 1231–1246, doi:10.1029/1999GB001229.

Letelier, R. M., J. E. Dore, C. D. Winn, and D. M. Karl (1996), Seasonal and interannual variations in photosynthetic carbon assimilation at Station ALOHA, *Deep Sea Res., Part II, 43*, 467–490, doi:10.1016/0967-0645(96)00006-9.

Luz, B., and E. Barkan (2000), Assessment of oceanic productivity with the triple-isotope composition of dissolved oxygen, *Science 288*, 2028–2031, doi: 10.1126/science.288.5473.2028.

Martin, A.P. (2003), Phytoplankton patchiness: the role of lateral stirring and mixing, *Progr. Oceanogr., 57*, 125–174, doi:10.1016/S0079-6611(03)00085-5.

Moisander, P. H., R. A. Beinart, M. Voss, and J. P. Zehr (2008), Diversity and abundance of diazotrophic microorganisms in the South China Sea during intermonsoon, *ISME J., 2*, 954–967, doi: 10.1038/ismej.2008.51.

McGillicuddy, D. (2001), The internal weather of the sea and its influences on ocean biogeochemistry, *Oceanogr., 14*, 78–92, doi:10.5670/oceanog.2001.09.

McGillicuddy, D. J., Jr., *et al*. (2007), Eddy/wind interactions stimulate extraordinary mid-ocean plankton blooms, *Science, 316*, 1021–1026, doi:10.1126/science.1136256.

Qiu, B., D. A. Koh, C. Lumpkin, and P. Flament (1997), Existence and formation mechanism of the North Hawaiian Ridge current, *J. Phys. Oceanogr., 27*, 431–444, doi:10.1175/1520-0485(1997)027<0431:EAFMOT>2.0.CO;2.

Quay, P. D., C. Peacock, K. Björkman, and D. M. Karl (2010), Measuring primary production rates in the ocean: Enigmatic results between incubation and non-incubation methods at Station ALOHA, *Global Biogeochem. Cycles, 24*, GB3014, doi:10.1029/2009GB003665.

Reuer, M. K., B. A. Barnett, M. L. Bender, P. G. Falkowski, and M. B. Hendricks (2007), New estimates of Southern Ocean biological production rates from O_2/Ar ratios and the triple isotope composition of O_2, *Deep Sea Res., Part I, 54*(6), 951–974, doi:910.1016/j.dsr.2007.1002.1007.

Riser, S. C., and K. S. Johnson (2008), Net production of oxygen in the subtropical oceans, *Nature, 451*, 323–325 doi:10.1038/nature06441.

Robidart, J. C., M. J. Church, J. P. Ryan, F. Ascani, S. T. Wilson, D. Bombar, R. Marin III, K. J. Richards, D. M. Karl, C. A. Scholin, and J. P. Zehr (2014), Ecogenomic sensor reveals controls on N_2-fixing microorganisms in the North Pacific Ocean, *ISME J., 8*, 1–11, doi:10.1038/ismej.2013.244

Roemmich, D., and J. Gilson (2009), The 2004-2008 mean and annual cycle of temperature, salinity, and steric height in the global ocean from the Argo Program. *Prog. Oceanogr, 82*, 81–100, doi: 10.1016/j.pocean.2009.03.004.

Suggett, D. J., K. Oxborough, N. R. Baker, H. L. MacIntyre, T. M. Kana, and R. J. Geider (2003), Fast repetition rate and pulse amplitude modulation chlorophyll a fluorescence measurements for assessment of photosynthetic electron transport in marine phytoplankton, *Eur. J. Phycol., 38*, 371–384, doi:10.1080/0967026031000161265 5.

Strickland, J. D. H., and T. R. Parsons (1972), *A Practical Handbook of Seawater Analysis*, 2nd ed., Fish. Res. Board of Can., Ottawa.

Tortell, P.D., E. C. Asher, H. W. Ducklow, J. A. L. Goldman, J. W. H. Dacey, J. J. Grzymski, J. N. Young, S. A. Kranz, K. S. Bernard, and F. M. M. Morel (2014), Metabolic balance of coastal Antarctic waters revealed by autonomous pCO_2 and O_2/Ar measurements, *Geophys. Res. Lett.*, *41*, 6803–6810, doi:10.1002/2014GL061266

Uitz, J., H. Claustre, A. Morel, and S. B. Hooker (2006), Vertical distribution of phytoplankton communities in open ocean: An assessment based on surface chlorophyll, *J. Geophys. Res.*, *111*(C8), doi:10.1029/2005JC003207.

Venrick, E. L. (1995), Scales of variability in a stable environment: phytoplankton in the central North Pacific, in Ecological time series, edited by T. M. Powell, and J. H. Steele, pp. 150–180, Chapman & Hall, NY.

Villareal, T. A., C. G. Brown, M. A. Brzezinski, J. W. Krause, and C. Wilson (2012), Summer diatom blooms in the North Pacific Subtropical Gyre: 2008–2009, *PLoS ONE*, *7*(4): e33109. doi:10.1371/journal.pone.0033109.

Wanninkhof, R. (2014), Relationship between wind speed and gas exchange over the ocean revisited, *Limnol. Oceanogr:Methods, 12*, 351–362, doi: 10.4319/lom.2014.12.351

Williams, R. G., and M. J. Follows (2011), Ocean Dynamics and the Carbon Cycle: Principles and Mechanisms, 404 pp., Cambridge Univ. Press, Cambridge, U. K.

Williams, P. J. le B., P.D. Quay, T. K. Westberry, and M. J. Behrenfeld (2013), The oligotrophic ocean is autotrophic, *Annu. Rev. Mar. Sci., 5*, 535–49, doi: 10.1146/annurev-marine-121211-172335.

Wilson, C. (2003), Late summer chlorophyll blooms in the oligotrophic North Pacific Subtropical Gyre, *Geophys. Res. Lett., 30*, 1942, doi:10.1029/2003GL017770.

Wilson, C., T. A. Villareal, M. A. Brzezinski, J. W. Krause, and A. Y. Shcherbina (2013), Chlorophyll bloom development and the subtropical front in the North Pacific, *J. Geophys. Res.*, *118*, 1473–1488, doi:10.1002/jgrc.20143.

Table 1. Oceanographic expeditions to Stn ALOHA between July to mid-September 2012

Cruise ID	Project	Dates
KM12-15	C-MORE	Jul 8 - 28
KM12-16	HOT-244	Jul 30 - Aug 3
KM12-17	C-MORE	Aug 5 - 14
KM12-18	HOT-245	Aug 16 - 20
KM12-19	C-MORE	Aug 22 - Sep 11

Table 2. Summary of productivity measurements conducted at Stn ALOHA during July and September 2012. The values represent MLD-integrated in units of mmol O_2 m^{-2} d^{-1} (using a conversion PQ of 1.1 for ^{14}C-assimilation which are also reported in units of carbon). The mean ± 1 standard deviation are shown for each set of measurements and absence of sample collection or calculation is indicated by not determined (n/d). The dates represent the start and end of each expedition and the number of samples is indicated by (*n*).

Method	8–28 Jul	5–14 Aug	22 Aug to 11 Sept
prior O_2/Ar-NCP	6.0 ± 3.2 (*n=16*)	-7.6 ± 4.2 (*n=8*)	-0.5 ± 3.1 (*n=16*)
real-time O_2/Ar-NCP	1.6 ± 2.6	3.9 ± 2.2	n/d
^{14}C-PP (carbon)	36.3 ± 6.5 (*n=16*)	26.7 ± 5.1 (*n=7*)	33.1 ± 7.4 (*n=16*)
(O_2)	39.9 ± 7.2	29.4 ± 5.5	36.4 ± 8.2
FRRF-PP	52.5 ± 13.2 (*n=17*)	n/d	52.7 ± 12.9 (*n=16*)
$^{17}\Delta O_2$-GPP	n/d	n/d	90.7 ± 35.3 (*n=22*)

FIGURES

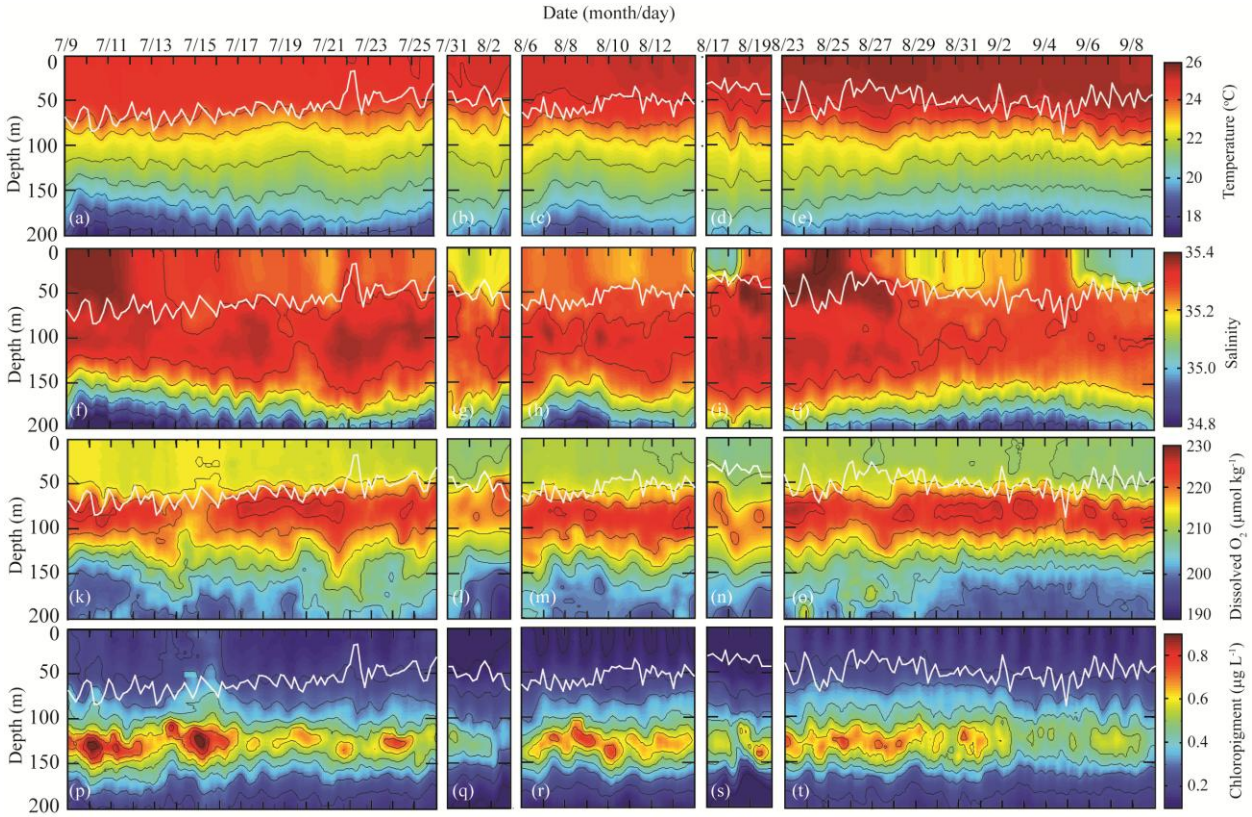

Figure 1. Upper water-column properties at Stn ALOHA during July-September 2012 showing (a-e) temperature, (f-j) salinity, (k-o) oxygen, and (p-t) chl*a* + phaeopigments. CTD profiles were conducted every 3 h during HOT cruises and every 4 h during C-MORE cruises (Table 1) and the white line represents the mixed layer depth.

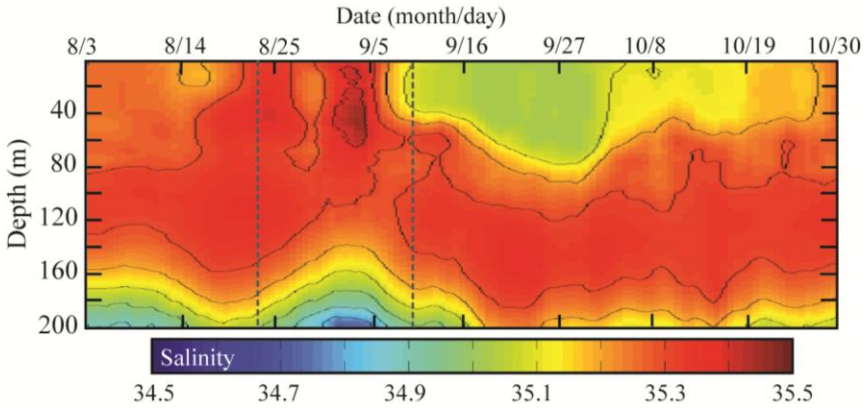

Figure 2. Upper water-column (0–200 m) profiles of salinity measured between 3 August and 30 October 2012 by a Seaglider. During September 2012, the Seaglider conducted 205 dives along ~370 km of the bowtie dive formation. The dashed lines indicate the time period when shipboard CTD profiles were conducted (shown in Figure 1f).

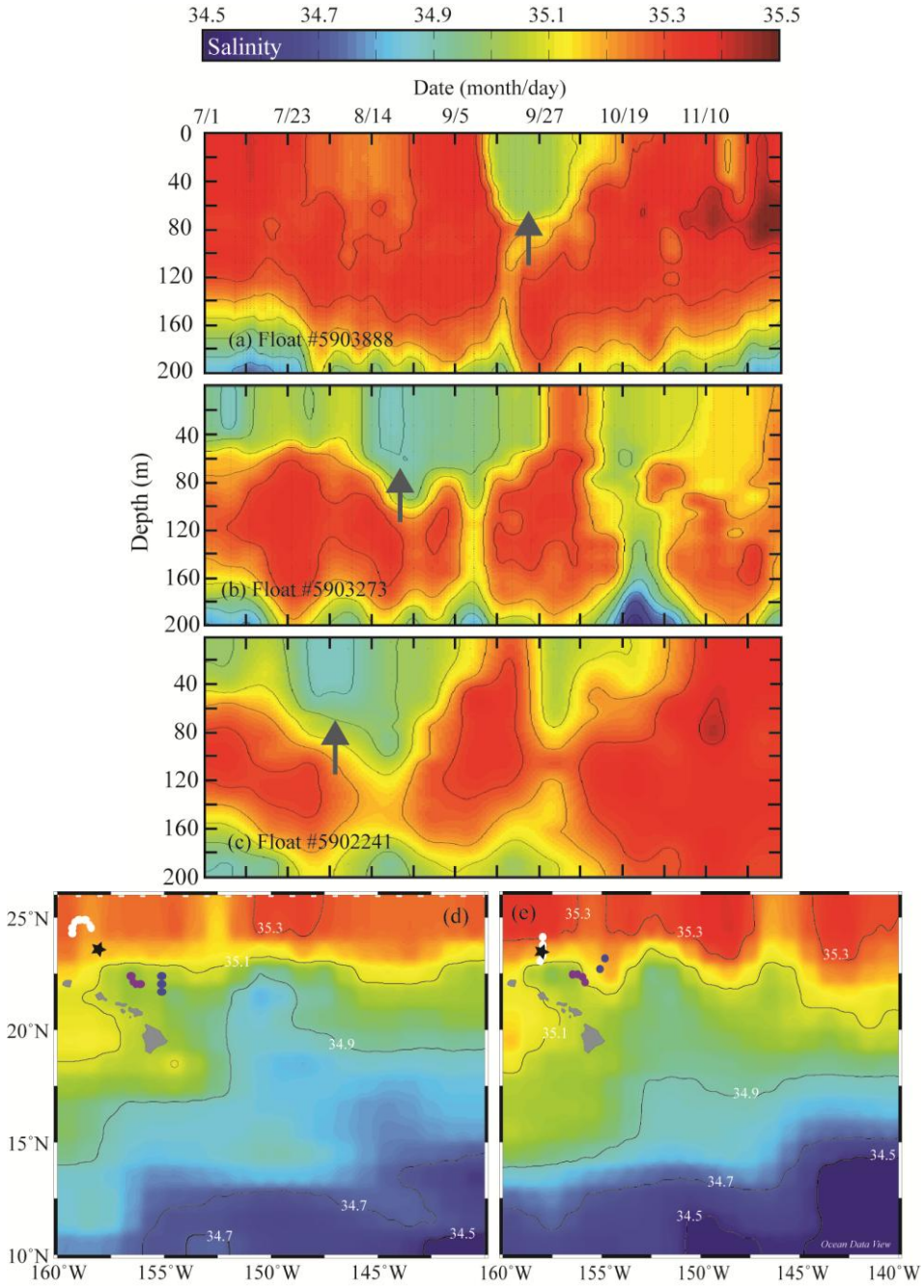

Figure 3. Figures 3a-c are salinity profiles from three Argo floats in the vicinity of Stn ALOHA between July and November 2012 (Roemmich and Gilson, 2009). The arrows represent surface salinity minimum features thought to correspond with the feature measured at Stn ALOHA in September 2012. Figures 3d-e are 0–100 m averaged salinity for August and September and include the position of the three Argo floats (#5903888 = white; #5903273 = purple, #5902241 = blue) in relation to the Hawaiian Islands and Stn ALOHA (shown by a star).

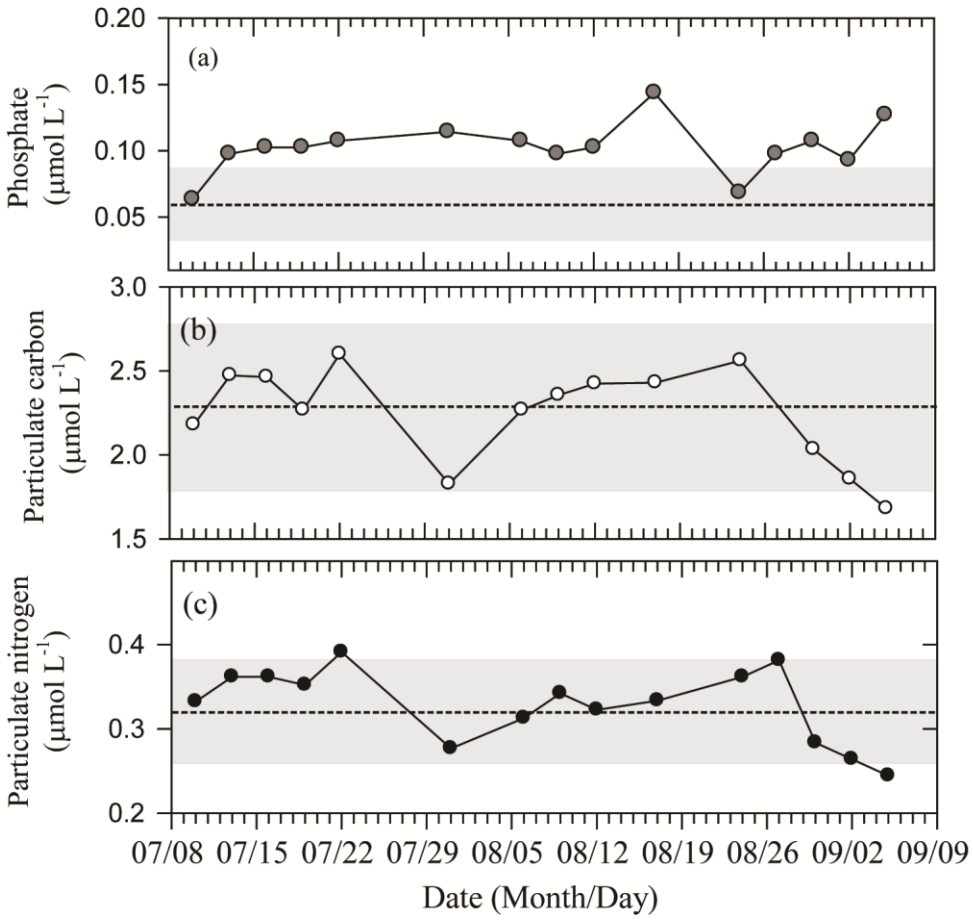

Figure 4. Depth-averaged (5–25 m) concentrations of (a) phosphate, (b) particulate carbon, and (c) particulate nitrogen during July-September 2012 at Stn ALOHA. The horizontal dashed line and shaded gray area represents the 5–25 m averaged mean concentration and standard deviation during 1989-2011 for the months of July-September.

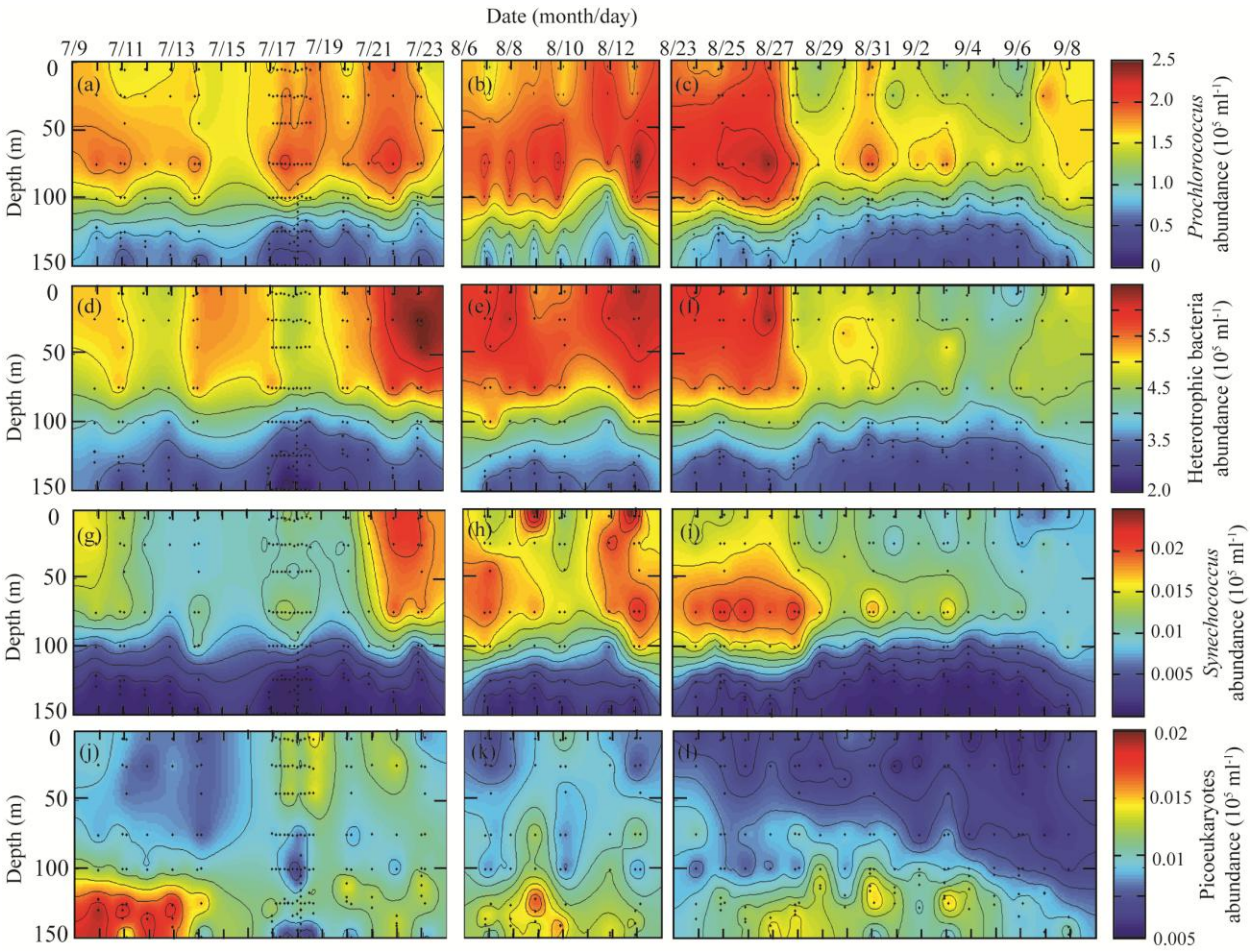

Figure 5. Depth profiles (0–150 m) of (a-c) *Prochlorococcus*, (d-f) heterotrophic bacteria, (g-i) *Synechococcus*, and (j-l) picoeukaryotes during July-September 2012 at Stn ALOHA.

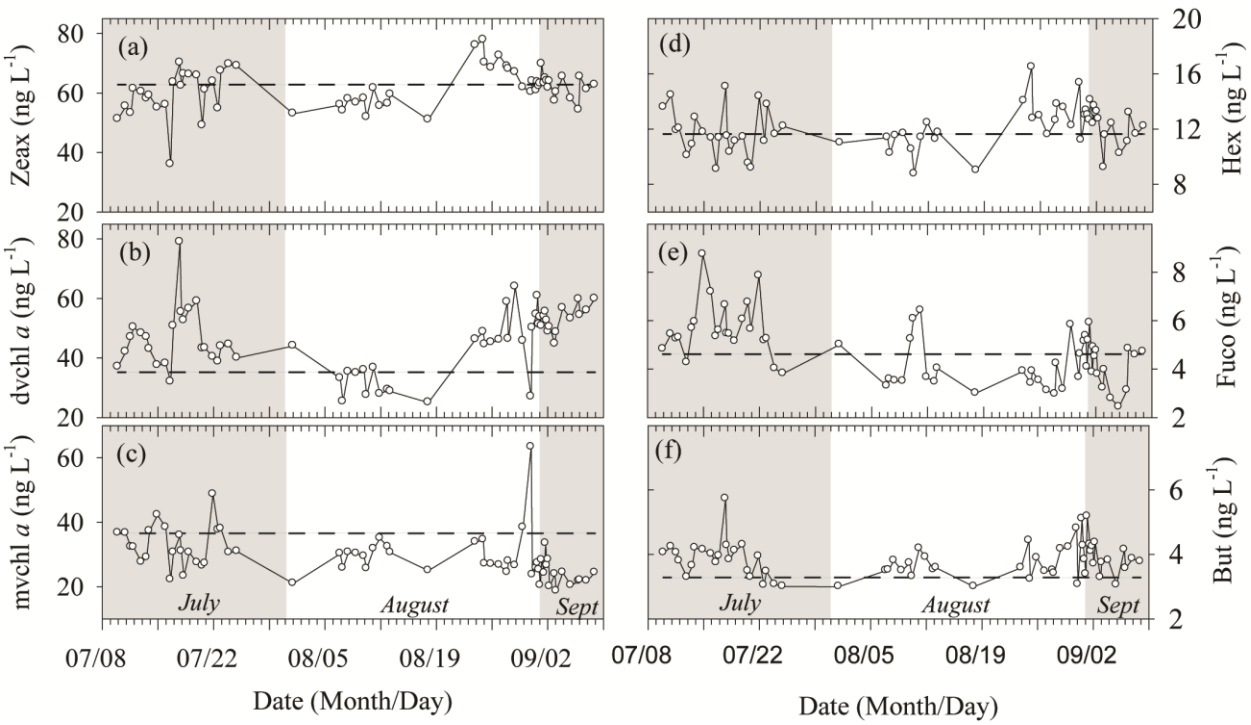

Figure 6. Temporal changes in depth averaged (5–25 m) concentrations of diagnostic pigment biomarkers including HOT data: (a) zeaxanthin, (b) divinylchlorophyll *a*, (c) monovinylchlorophyll *a* (d) 19′-hexanoyloxyfucoxanthin, (e) fucoxanthin, and (f) 19′-butanoyloxyfucoxanthin. The horizontal dashed line represents the mean concentration for each respective pigment averaged for July-September using the 1989–2011 HOT climatological record.

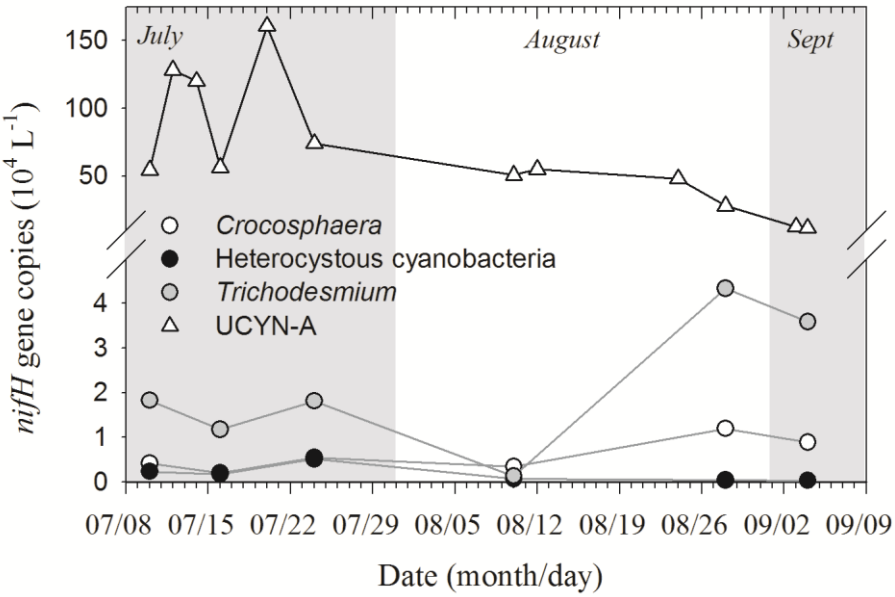

1092

1093 **Figure 7**. Depth averaged (5–25 m) *nifH* gene copies during July-September 2012 for four major

1094 groups of diazotrophs: UCYN-A, *Crocosphaera*, heterocystous cyanobacteria, and

1095 *Trichodesmium*.

1096

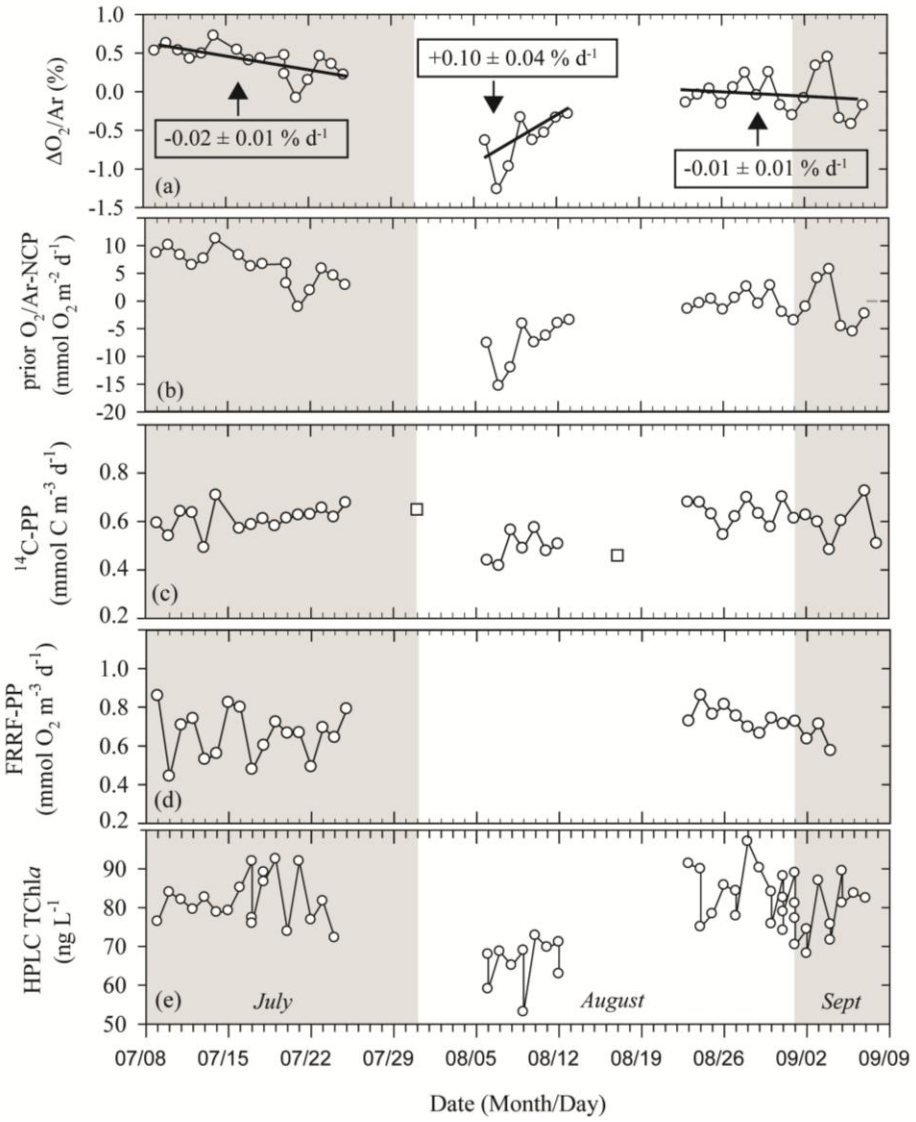

Figure 8. Productivity and TChl*a* at Stn ALOHA during July to September 2012: (a) $\Delta O_2/Ar$ (%), (b) prior O_2/Ar-NCP, (c) ^{14}C-PP including HOT data as square symbols, (d) FRRF-PP, and (e) TChl*a*. The samples were collected at a depth of 25 m and the gray shaded areas indicate months of year.

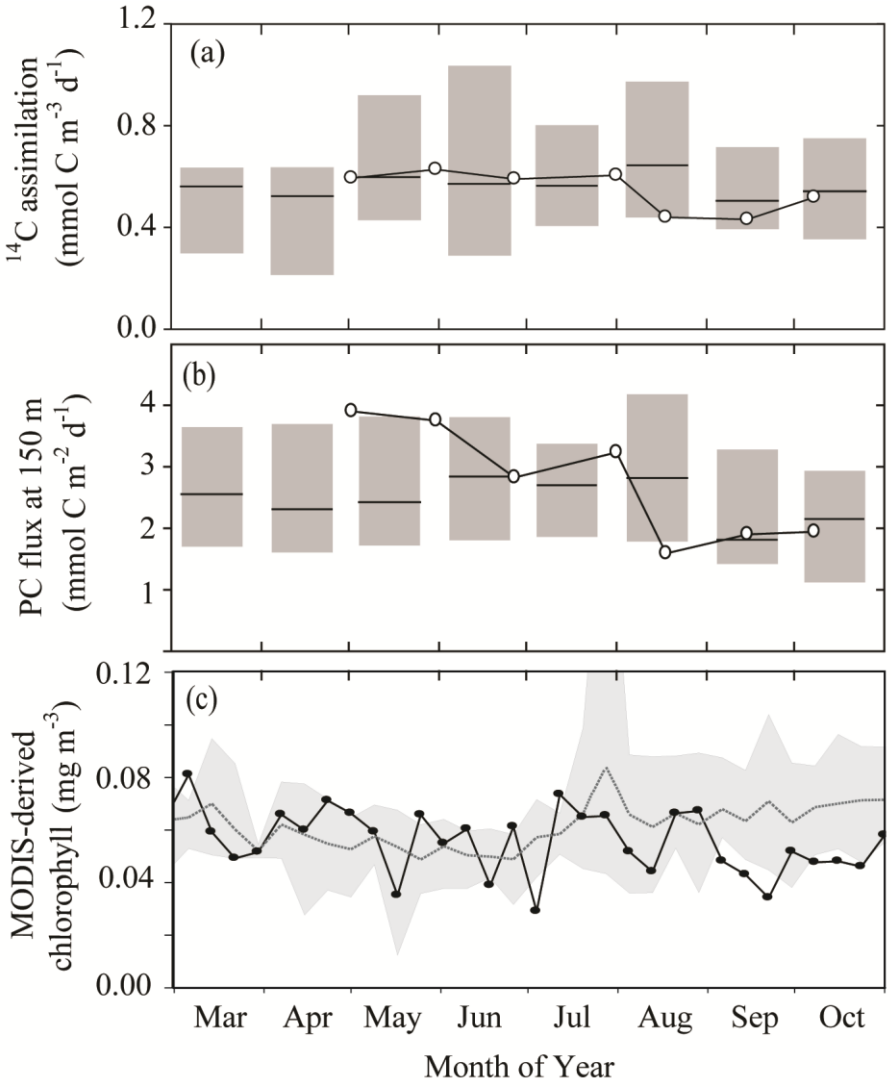

Figure 9. Comparison of key parameters in March-October 2012 with historical data. Figure 9(a) ^{14}C-PP productivity (5–25 m depth-averaged) and (b) particulate carbon flux measured at 150 m during March-October 2012 with 1989–2011 climatology. The values measured in 2012 are shown as white circles. The 1989–2011 data are binned by month and are shown as gray bars with the upper and lower boundaries represented by the 5 and 95 percentile and the mean value for each month shown by the horizontal black line. Figure 9(c) Comparison of MODIS-derived chlorophyll *a* concentrations at Stn ALOHA in March-October 2012 with 2002–2014. The 2012 values are shown by a solid black line and closed circles, the 2002-2014 values are represented by the dashed gray line (mean) and the shaded gray area (minimum and maximum)

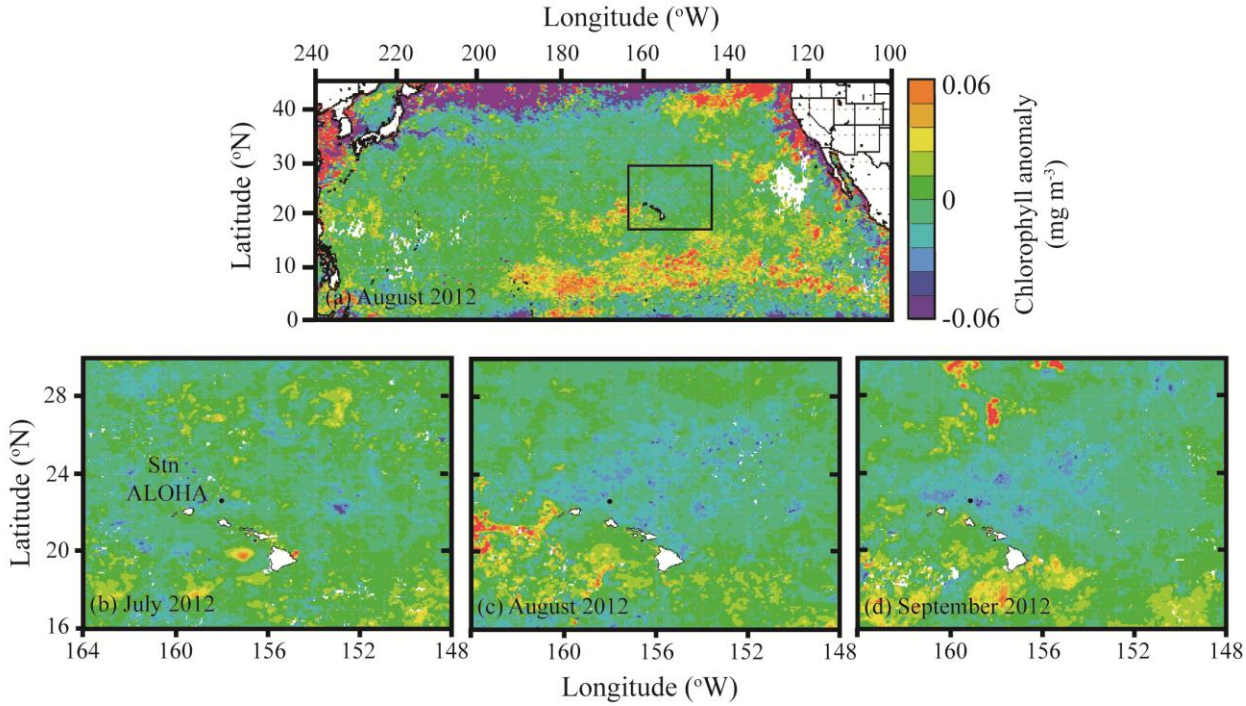

Figure 10. Anomaly of chlorophyll *a* concentration during August 2012 for (a) North Pacific Ocean and Stn ALOHA and the vicinity during (b) July, (c) August, and (d) September 2012. The box drawn around the Hawaiian Islands (Figure 12a) corresponds to the latitude and longitude shown in Figures 12b-d.